Ammonium sensitivity of biological nitrogen fixation in anaerobic diazotrophs and coastal salt marsh sediments

Romain Darnajoux[1], Linta Reji[2], Xinrei Zhang[2], Katja Edeltrud Luxem[2], and Xinning Zhang[3]

[1]Princeton University, Dept. of Geosciences
[2]Princeton University
[3]Princeton Univ, Dept Geosci, Guyot Hall, Princeton, NJ 08544 USA

November 24, 2022

Abstract

New bioavailable nitrogen (N) from biological nitrogen fixation (BNF) is critical for the N budget and productivity of marine ecosystems. Nitrogen-fixing organisms typically inactivate BNF when less metabolically costly N sources, like ammonium (NH4+), are available. Yet, several studies observed BNF in benthic marine sediments linked to anaerobic sulfate-reducing bacteria (SRB) and fermenting firmicutes despite high porewater NH4+;concentrations (10-1,500 μM), making the importance of and regulating controls on benthic BNF unclear. Here, we evaluate BNF sensitivity to NH4+ in model anaerobic diazotrophs, the sulfate-reducer Desulfovibrio vulgaris var. Hildenborough and fermenter Clostridium pasteurianum strain W5; in sulfate-reducing sediment enrichment cultures, and in sediment slurry incubations from three Northeastern salt marshes (USA). BNF in sulfate-reducing cultures and sediments is highly sensitive to external NH4+, with a threshold for BNF inhibition of [NH4+] $<$ 2 μM in cultures and $<$ 9 μM in sediment slurries. The prevalence of SRB-like sequences in sediment-derived nitrogenase (nifH) genes and transcripts in this and other studies of benthic BNF along with an analysis of benthic NH4+ porewater data suggests a broad applicability of the inhibition thresholds measured here and the confinement of benthic BNF to surficial sediments. The timing of inhibition, fast NH4+ drawdown, and sediment heterogeneity are factors that can complicate studies of benthic BNF sensitivity to NH4+. We propose a simple theoretical framework based on the affinity of the NH4+ transporter to explain NH4+ control of BNF and improve biogeochemical models of N cycling.

Ammonium sensitivity of biological nitrogen fixation in anaerobic diazotrophs and coastal salt marsh sediments.

Romain Darnajoux[1], Linta Reji[1], Xin Rei Zhang[1,2], Katja E. Luxem[1], and Xinning Zhang[1, 2]

[1]Department of Geosciences, Princeton University, Princeton, 08544, NJ, USA

[2]High Meadows Environmental Institute, Princeton University, Princeton, 08544, NJ, USA

Corresponding author: RD and XZ

ORCID: RD: 0000-0002-4996-0067, XZ: 0000-0003-2763-1526, KEL: 0000-0001-7310-0668, LR: 0000-0002-1337-6782

Key points:

- We identified a porewater ammonium concentration threshold of 9 µM for biological nitrogen fixation inhibition in benthic environments.
- Drawdown of porewater ammonium, timing of enzyme inhibition, and sediment heterogeneity can complicate measurement of nitrogen sensitivity.
- Review of porewater ammonium concentration indicates biological nitrogen fixation is likely limited to the superficial layer of sediments.

Abstract:

New bioavailable nitrogen (N) from biological nitrogen fixation (BNF) is critical for the N budget and productivity of marine ecosystems. Nitrogen-fixing organisms typically inactivate BNF when less metabolically costly N sources, like ammonium (NH_4^+), are available. Yet, several studies observed BNF in benthic marine sediments linked to anaerobic sulfate-reducing bacteria (SRB) and fermenting firmicutes despite high porewater NH_4^+ concentrations (10-1,500 µM), making the importance of and regulating controls on benthic BNF unclear. Here, we evaluate BNF sensitivity to NH_4^+ in model anaerobic diazotrophs, the sulfate-reducer *Desulfovibrio vulgaris* var. Hildenborough and fermenter *Clostridium pasteurianum* strain W5; in sulfate-reducing sediment enrichment cultures, and in sediment slurry incubations from three Northeastern salt marshes (USA). BNF in sulfate-reducing cultures and sediments is highly sensitive to external NH_4^+, with a threshold for BNF inhibition of $[NH_4^+] < 2$ µM in cultures and < 9 µM in sediment slurries. The prevalence of SRB-like sequences in sediment-derived nitrogenase (*nifH*) genes and transcripts in this and other studies of benthic BNF along with an analysis of benthic NH_4^+ porewater data suggests a broad applicability of the inhibition thresholds measured here and the confinement of benthic BNF to surficial sediments. The timing of inhibition, fast NH_4^+ drawdown, and sediment heterogeneity are factors that can complicate studies of benthic BNF sensitivity to NH_4^+. We propose a simple theoretical framework based on the affinity of the NH_4^+ transporter to explain NH_4^+ control of BNF and improve biogeochemical models of N cycling.

Introduction

The requirement for bioavailable fixed nitrogen (N) is a fundamental constraint for all life on Earth. Biological nitrogen fixation (BNF), the only biological process capable of producing newly fixed N, is critical for the function and ecology of the biosphere. Present in a small subset of taxonomically and metabolically diverse prokaryotes termed diazotrophs, all BNF is catalyzed by the enzyme nitrogenase in a complex, energy-intensive reaction that reduces dinitrogen (N_2) into ammonia (NH_3), which is subsequently incorporated into cell material. Diazotrophs thus function as natural gatekeepers for ecosystem N input and are particularly important in oligotrophic systems, such as the surface waters of the tropical and subtropical ocean (Sohm et al., 2011; Voss et al., 2013; Zehr & Kudela, 2011), where low, nanomolar levels of dissolved inorganic fixed N species (DIN *i.e.*, ammonium NH_4^+, nitrite NO_2^-, nitrate NO_3^-) limit primary production (Elser et al., 2007).

The distribution of BNF in marine waters was traditionally explained by the well-documented regulation of nitrogenase synthesis and activity by DIN in model cyanobacterial and aerobic diazotrophs (*e.g.*, *Trichodesmium* and *Azotobacter*), which downregulate BNF when ambient DIN concentrations are sufficient to meet cell anabolic demands (*e.g.*, external [NH_4^+] > hundreds of nanomolar to tens of micromolar, depending on the species (Drozd et al., 1972; Hartmann et al., 1986; Holl & Montoya, 2005; Kleiner, 1974; Mulholland et al., 2001; Ohki et al., 1991; Postgate & Kent, 1984). This downregulation reflects the high energetic cost of N acquisition through BNF, in comparison to the metabolic cost of assimilating NH_4^+ or NO_3^- (Glibert et al., 2016; Großkopf & LaRoche, 2012; Inomura et al., 2017). Accordingly, marine BNF in hypoxic and anoxic benthic environments, where porewater NH_4^+ concentrations are typically orders of magnitude higher than in euphotic zones (see Knapp and reference therein) (Knapp, 2012), has been estimated to account for only 10% of total marine new N inputs, with benthic BNF largely restricted to highly productive shallow sedimentary environments like seagrass meadows (Capone, 1988; Capone & Carpenter, 1982; Zhang et al., 2020).

However, recent studies ranging from open ocean to coastal estuary benthic systems have challenged the above paradigm based on observations of BNF activity and nitrogenase (*nifH, nitrogenase reductase*) genes and transcripts in sediments with high porewater NH_4^+ concentrations (e.g. ~ 50-1500 μM) (Bertics et al., 2013; Gier et al., 2016; Knapp, 2012). These results, many obtained with closed vessel sediment incubation experiments, have led to the proposal that benthic BNF may be a larger contribution to marine N inputs than previously thought (Fulweiler et al., 2007; Newell, McCarthy, et al., 2016; David T. Welsh, 2000). At a larger scale, increased benthic BNF has been suggested to help resolve an apparent and highly debated imbalance in the modern marine N budget (Codispoti, 2007; Gruber & Galloway, 2008; Zhang et al., 2020). A better understanding of the ecophysiology of benthic diazotrophs, particularly how such microorganisms regulate BNF under fluctuating environmental conditions, is necessary to resolve questions of when and why BNF occurs in benthic settings and to ascertain its importance to the marine N cycle.

Molecular surveys of the nitrogenase gene *nifH* (Bertics et al., 2010; Kapili et al., 2020; Newell, Pritchard, et al., 2016; Zehr et al., 2003) and activity assays designed to target specific microbial groups (*e.g.*, molybdate additions, sulfide production) (Bertics et al., 2010; Gandy & Yoch, 1988; Newell, Pritchard, et al., 2016; D. T. Welsh et al., 1996) have identified sulfate-reducing bacteria (SRB), such as *Desulfovibrio* sp., as the dominant N_2 fixers in benthic systems (Brown & Jenkins, 2014; Dekas et al., 2018; Gier et al., 2015; Kapili et al., 2020; Newell, McCarthy, et al., 2016). Fermentative firmicute species (*e.g*. *Clostridium* sp.) have also been consistently observed in surveys of benthic diazotrophy (Gier et al., 2016; Kapili et al., 2020). Such data, which imply a very low sensitivity of BNF to DIN in SRB and Clostridia, have been used to suggest that the physiology and purpose of BNF in benthic organisms could be fundamentally different from that of euphotic zone N_2 fixers (Knapp, 2012). For example, BNF at high NH_4^+ (*e.g*. $[NH_4^+] > 50$ μM) has been taken as a sign that benthic microorganisms may be using BNF to balance intracellular redox under reducing conditions (Tichi & Tabita, 2000). While this paradox has important implications for our

98 understanding of marine N cycling, the physiologies of N_2 fixation in SRB and other anaerobic
99 diazotrophs have garnered little attention compared to the aerobic and phototrophic
100 diazotrophs (Gordon et al., 1981; Postgate & Kent, 1984; Riederer-Henderson & Wilson,
101 1970; Tubb & Postgate, 1973).

102 Here, we examine N_2 fixation by the model SRB *Desulfovibrio vulgaris* var.
103 Hildenborough (*Dv*H) (Heidelberg et al., 2004) and the model fermenter *Clostridium*
104 *pasteurianum* strain W5 (*Cp*) (Winogradsky, 1895), two free-living diazotrophic species
105 common in sediments (Brown & Jenkins, 2014), and in sulfate-reducing sediments from
106 three salt marshes along the Northeastern coast of the United States. By simultaneously
107 tracking BNF activity and ambient NH_4^+ concentrations in liquid culture incubations, we find
108 that BNF by *Dv*H only occurs once NH_4^+ concentrations fall below ~ 2 µM and < 20 µM in *Cp*,
109 where we had lower data resolution. In sediment slurry incubations assayed using two
110 independent methods (acetylene reduction assay and ^{15}N tracer), the NH_4^+ threshold for
111 BNF inhibition is ~ 9 µM. The data indicate benthic BNF is more sensitive to fixed N than
112 recent studies would suggest and similar to the NH_4^+ sensitivity of BNF by diverse cultured
113 diazotrophs. Analyses of nitrogen fixation genes and porewater NH_4^+ data suggest the broad
114 relevance of the ammonium threshold measured. We find that the timing of BNF inhibition by
115 NH_4^+, the fast removal of ambient NH_4^+ by active microorganisms, and the heterogeneous
116 nature of sediments must be considered when investigating the NH_4^+ sensitivity of BNF,
117 particularly with incubation experiments. To improve mechanistic models of N
118 biogeochemistry, we propose a simple theoretical framework based on ammonium
119 transporter kinetics to link ambient porewater NH_4^+ concentrations to BNF activity.

120 **Material and Methods**

121 *Culture conditions*

122 *Desulfovibrio vulgaris var. Hildenborough* (ATCC 29579), (Heidelberg et al., 2004) was
123 grown anaerobically in minimal diazotrophic media for sulfate reducers using a recipe

modified from Sim et al., 2013 in 27 mL Balch tubes (10 mL media) or 160 mL serum vial (50 mL media) with 20 mm butyl rubber septum stoppers (Bellco glass, Vineland, NJ, USA). Medium modifications include the use of 0.07g.L^{-1} ascorbate in place of titanium citrate as the reductant and the omission of tungstate from the trace metal mix. Media was prepared using standard anoxic procedures and a glovebox (Coy Laboratories, Grass Lake, MI, USA). Resazurin (1mg.L^{-1}) was used to monitor shifts in the redox potential of the medium during our experiments. Sulfate (Na_2SO_4) was provided as an electron acceptor at 30 mM. Pyruvate or sodium lactate (30 mM), used as the carbon and electron sources, were the growth limiting nutrients. Sterilization was performed by autoclaving individual tubes for a minimum of 15 min at 120^{o}C. The final pH of the media was 7.3 $\pm$ 0.1. Cells were grown at 30^{o}C in the dark, with tubes placed obliquely in an orbital shaker at a constant agitation speed of 130 rpm. *Clostridium pasteurianum* strain W5 was obtained from the DSMZ (German Collection of Microorganisms and Cell Cultures, Braunschweig, Germany). The cells were grown in a diazotrophic media with sucrose as the fermentative substrate as described in Westlake & Wilson, 1959, in 27 mL Balch tubes (10 mL culture) sealed with 20 mm butyl rubber stoppers (Bellco glass, Vineland, NJ, USA) and aluminum seals. Media tubes were sterilized by autoclaving at 121^{o}C for 45 minutes. Final pH of the media was 6.8. Cells were grown at 30^{o}C in the dark, with constant orbital shaking at 100 rpm. Culture cell density was followed by turbidimetry at OD 600 nm using a Thermo Fisher Scientific (Waltham, MA, USA) GENESYS spectrophotometer equipped with a tube holder. Anoxic transfer of NH_4^+ as ammonium chloride was accomplished using syringes and needles from 10- to 100-fold stock solutions prepared in culture media.

Slurry incubations of salt marsh sediments.

Samples of salt marsh sediments (Table 1) were collected from Barnegat Bay in New Jersey (denoted here as “NJ” saltmarsh, Lat: 40.031319, Long: -74.080609), the Sippewissett Salt Marsh in Massachusetts (denoted here as “MA” saltmarsh, Lat: 41.590533, Long: -70.639711) and from Great Bay in New Hampshire (denoted here as “NH” saltmarsh, Lat:

43.125, Long: -70.868). Sediments were kept at 4^{o}C in the dark until being processed in the laboratory. To determine sediment BNF sensitivity to NH_4^+, 20 $\pm$ 1g of wet sediment was introduced in a 260 mL serum bottle and acclimated in an anoxic glove bag (2% H_2 98% N_2) overnight for each incubation. On the day of the experiment, 80 mL of SRB minimal media (described above) containing 30 mM lactate and 30mM SO_4^{2-} was added to each sample prior to sealing the bottle. Each experiment had 10 replicates for each condition (NJ, n = 2; NH and MA, n = 4) where ambient NH_4^+ concentrations and BNF activity (^{15}N and Acetylene Reduction Activity, see methods below) were measured simultaneously. Samples were incubated in the dark in an orbital shaker at 30 ^{o}C (ARA) and 26 ^{o}C (^{15}N) with constant agitation (100 rpm). Six of the ten sediment samples assayed by ^{15}N received initial addition of ammonium (~300 µM final concentration) before starting the experiments. After the initial onset of BNF, we added NH_4^+ (~300 µM final concentration) in all but two samples (ARA, NJ).

Enrichment of sulfate-reducing bacteria

Small amounts of sediment (~1 g) from the Barnegat Bay salt marsh were introduced into 60 mL serum bottles containing SRB-minimum media (prepared as described above). Initial enrichments were sequentially transferred into fresh DIN-free media at least 6 times before BNF sensitivity experiments. SRBB1 and SRBB2 enrichment cultures were grown under the same conditions as strain *Dv*H. Identity and purity of the enrichment consortia (NCBI accessions will be added upon acceptance of the manuscript) were determined using 16S rRNA and *nifH* genes.

Evaluation of N_2 fixation activity.

To avoid its inhibitory effects, a lower acetylene concentration (~ 2.5 % instead of 10%) than typically used in the traditional Acetylene Reduction Assay (ARA) (Hardy et al., 1968) was employed to assess changes in BNF activity by *Dv*H and *Cp* cultures and sulfate-reducing sediments. An experiment was started when culture at the beginning of exponential growth

(OD_{600} ~ 0.09 for *Dv*H and ~ 0.1 for *Cp*, Supplementary Figs. S3 and S4) by replacing ~ 2.5 % of the total headspace (2.4-2.7%, depending on vessel volume) with 100% acetylene generated anaerobically with N_2 background in a serum bottle from technical grade calcium carbide (Sigma Aldrich, St Louis, MO, USA). At each time point, 1-3 mL of the headspace was exchanged with the same volume of ~2.5% acetylene in N_2 and stored in a 3 mL Exetainer ® vial (Labco, Lampeter, UK). Acetylene Reduction (AR) activity was evaluated by measuring ethylene concentration in the headspace at different times using a Shimadzu (Kyoto, Japan) 8A GC-FID as previously described (Bellenger et al., 2011). Results were corrected for the sequential dilution of the headspace during resampling.

Direct nitrogen fixation activity was determined by measuring ^{15}N incorporation into biomass from $^{30}N_2$ (Montoya et al., 1996). Briefly, the ^{15}N tracer experiment was started by replacing 20% of the headspace and liquid phase with $^{30}N_2$ gas (98%+ v/v, Cambridge Isotope laboratories, Andover, MA, USA) and media equilibrated with $^{30}N_2$ gas, respectively (Mohr et al., 2010). At each time point, 3-4 mL of sediment slurry or cell culture was sampled and centrifuged at 8000 rpm. Supernatant was filtered and used for NH_4^+ measurement (see below) and solid samples were stored at -20^{o}C until further processing. Solid sediments samples were then dried and weighed, and a known amount was sent for ^{15}N and ^{13}C analyses at UC Davis Stable Isotopes Facility (https://stableisotopefacility.ucdavis.edu).

Measurement of ammonium concentration.

At every time point for assessing BNF activity by ARA or the ^{15}N tracer method, 1-3mL of supernatant was removed from the incubation and filter-sterilized (0.2 µm hydrophilic PTFE or PES syringe filters, Agilent Technologies and MilliporeSigma, respectively). Filtered samples, procedural blanks, and freshly prepared NH_4^+ chloride standards (0.8 µM - 0.1 M) for NH_4^+ analysis were then stored at -20^{o}C until further processing. Ammonium was measured by fluorescence using the o-phthalaldehyde (OPA) method (Holmes et al., 1999). Under our conditions, uncertainty for [NH_4^+] in the range of 0-10 µM was estimated using

duplicate measurements over 3 different days (n=20) and found to be 1.3 µM. Several filtered supernatant aliquots representing several timepoints sampled from five sediment incubations assessed by ARA (#4, #6, #7, #9, #10) after NH_4^+ addition exhibited irregular coloration (red-black instead of yellow) during the OPA procedure, even after 8-fold dilution (Supplementary Fig. S2). After careful examination (see Supplementary Material Sup. Discussion), these measurements (highlighted with red stars in Fig. 3 and Supplementary Fig. S5) were disregarded for the purpose of this study. To determine the NH_4^+ threshold for BNF inhibition (see Fig. 3), several NH_4^+ concentrations were averaged over two time-points to link BNF rate and NH_4^+ concentration, without significant influence on the statistical determination of $[NH_4^+]_{95\%}$ threshold value estimates.

Review of porewater ammonium concentration in sediments.

To estimate the extent to which sediment porewater ammonium concentrations reach the ammonium threshold for BNF inhibition at the global scale, we extracted porewater ammonium concentrations and depth gradients from 26 studies representing 5 continents (Europe, North America, South America, Asia, and Oceania). We reviewed all benthic references included in Knapp et al. 2012, as well as several references reporting BNF at high $[NH_4^+]$. We further identified more recent publications using a keyword search in Google Scholar, searching for "'ammonium concentration sediments pore water coastal" and filtering the results to include studies published after 2012 (Supplementary Table S1). Papers were manually inspected, and ammonium concentrations when present were collected from tables or estimated from direct graphic reading when no tabulated values were available (~ 10% or 5 µM of reading uncertainty, whichever was larger). For each sediment dataset, we derived the general shape of the depth gradient of porewater ammonium (*i.e.*, depth and $[NH_4^+]$ values were extracted at initial, break in slope, plateau, and maximal measurement depths). For the value of ammonium concentration at 0 cm (sediment/water interface), the value reported in the study, $[NH_4^+]$ of the overlying water, or 0 µM was used, in this order of preference. We then applied a linear interpolation to estimate the depth at which the

porewater concentration was equal to our threshold (*i.e*. threshold depth). When data were presented as an average value for the whole sample or sediment core, the average porewater [NH_4^+] was attributed to the average depth (i.e., half the maximal depth of sampling) before interpolation.

Extraction and analysis of nucleic acid sequence from salt marsh sediments.

At the end of the ARA and ^{15}N incubations, 3 mL of slurry was removed from the samples, centrifuged at 5000 g, resuspended in LifeGuard® Soil Preservation solution (Qiagen, Germantown, MD, USA) and stored at -20°C. DNA and RNA extraction were conducted using the RNEasy PowerSoil® Total RNA and DNA elution kit (Invitrogen, Carlsbad, CA, USA) following the recommendation of the supplier and extracts were stored at -80°C. Nucleic acid purity was assessed using NanoDrop (Thermo Fisher Scientific) and Qubit® (Thermo Fisher Scientific) measurements. RNA samples were converted into cDNA using the SuperScript ® IV First Strand kit (Invitrogen) following the recommendation of the supplier. Nested PCR amplification of *nifH* genes from DNA and cDNA were conducted in triplicate according to the modified protocol of Zehr et al., 1998 from Jayakumar et al., 2017. Amplification was verified by gel electrophoresis and amplicons from cDNA were pooled and sent with total DNA extract for *nifH* and 16S rRNA gene sequencing using bTEFAP ® and Illumina MiSeq300 at the MRDNA ® facility (Shallowater, TX, USA). 16S rRNA genes were sequenced using 515f/806r primer pair targeting the V4 region (Caporaso et al., 2012), and *nifH* genes were sequenced with the nifH1/nifH2 primer pair (Zehr & McReynolds, 1989). The commercial in-house data processing pipeline at MRDNA® was used to process the sequence data and cluster OTUs (97% similarity threshold). OTUs were taxonomically classified against a curated database derived from the Ribosomal Database Project Release 11 (RDPII) for the 16S rRNA gene and the NCBI non-redundant nucleotide sequences database for *nifH*.

We pruned the sequence datasets to retain only OTUs with absolute abundance > 1 000 counts and relative abundance > 0.2%. The top 500 *nifH* gene OTUs and the pruned transcript OTUs (n=55) from ARA and ^{15}N incubations, as well as *nifH* gene OTUs (n=46) from our two salt marsh enrichments SRBB1 and SRBB2 were aligned against a representative (*i.e.*, all major *nifH* groups represented) subset (n=152) of *nifH* database recently curated in a deep sea sediment study (Kapili et al., 2020). Aligned sequences (see Fig. 4A) were then separated into gene (after pruning, n=59) and transcript datasets to build individual maximum-likelihood phylogenetic trees using FastTree (v2.1.11, GTR+CAT model, 1,000 resamples, Price et al., 2010). Data processing and visualizations were conducted using R Studio (v1.3.1056) and R (v4.0.3) using the *phyloseq* (v.1.32.0) (McMurdie & Holmes, 2013) and *ggtree* (v2.2.4) packages. Hierarchical clustering (*stat* v4.0.3, method Ward.D2) was conducted on *clr*-transformed relative abundance data (Gloor et al., 2017) using the package *compositions* (v2.0-0) (van den Boogaart & Tolosana-Delgado, 2008). Canonical Analysis of Principal coordinate (CAP, 45) were performed on OTUs abundance data using Bray-Curtis dissimilarity, and a Redundancy Analysis (RDA as implemented in vegan v2.5-6,Oksanen et al., 2019) was conducted on normalized geochemical data. It is worth noting that we were still able to find *nifH* sequences in the reagent blank control, indicating contamination (Goto et al., 2005; Zehr et al., 2003) or cross-contamination between samples during extraction or sequencing. In particular, two-three sediment slurry samples, characterized by low DNA concentration, purity, and a low number of sequences (< 50 000 counts, Fig. 4B), cluster with our control sequence data, indicating they might be disproportionately affected by contamination (purple box in Fig. 4B top panel and Fig. 5B).

Results

Growth rates and yields of Desulfovibrio vulgaris and Clostridium pasteurianum under diazotrophic and ammoniotrophic conditions

We compared the growth of the two models anaerobic diazotrophs *D. vulgaris* var Hildenborough (strain *Dv*H) and *Clostridium pasteurianum* (*Cp*) under fully diazotrophic and NH_4^+ replete conditions (Fig. 1A and B). For *Dv*H, as expected for diazotrophs, including SRB (Lespinat et al., 1987), diazotrophic growth (μ_{N2} = 0.046 ± 0.005 h^{-1}, SE n=3) was much slower (~ 2-fold) than NH_4^+ replete growth (μ_{NH4+} = 0.10 ± 0.004 h^{-1}, SE, n=3), compatible with the typically higher energetic costs of BNF compared to NH_4^+ usage for N anabolism (Inomura et al., 2017). Biomass yields ($OD_{Max,NH4+}$ = 0.82 ± 0.02 vs. $OD_{Max,N2}$ = 0.39 ± 0.01, SE n=3, Fig. 1A) also support this interpretation. Growth at sub-replete initial NH_4^+ concentrations under our culture conditions (*e.g.*, [NH_4^+] = 500 µM, 30 mM pyruvate, 30 mM sulfate, Fig. 1A) showed clear biphasic growth, with a first exponential growth phase (µ = 0.094 h^{-1}), a second lag phase of ~ 50 h, and a second short exponential growth phase (µ ~ 0.007 h^{-1}), all being consistent with a transition from ammoniotrophic to diazotrophic growth as medium NH_4^+ becomes depleted. Accordingly, no BNF activity as measured by ethylene production by ARA was detected during ammoniotrophic growth in similar experiments (data not shown).

Clostridium pasteurianum grown fermentatively on sucrose exhibited a shorter lag-phase than *Dv*H regardless of N status (5h for *Cp* vs 50h for *Dv*H, Fig. 1B). *Clostridium pasteurianum* grew 1.5-fold slower under diazotrophic conditions (μ_{N2} = 0.238 ± 0.006 h^{-1}, SE n=3) (Fig. 1B) than during NH_4^+ replete growth (μ_{NH4+} = 0.358 ± 0.002 h^{-1}, SE n=3). While the slower growth and lower biomass yield of diazotrophy relative to ammoniotrophy by *Cp* ($OD_{Max,NH4+}$ = 1.6 ± 0.02 vs. $OD_{Max,N2}$ = 1.3 ± 0.01, SE n=3, Fig. 1B) demonstrate the higher metabolic cost of N acquisition by BNF during fermentative growth, the differences are not as large as observed for sulfate reducing *Dv*H. The faster growth of *Cp* relative to *Dv*H corresponded with a very fast and barely measurable transition (~ 1 h for *Cp* vs 50 h *Dv*H) between ammoniotrophic and diazotrophic growth regimes, which was induced by initial growth on sub-replete ammonium levels (Fig. 1B).

307 *BNF dependency on timing and concentration of ammonium additions to N_2-fixing pure*
308 *cultures*

309 To study the response of BNF to extracellular NH_4^+, we performed NH_4^+ addition
310 experiments on the slower growing *Dv*H acclimated to fully N_2-fixing conditions (no NH_4^+
311 addition, Fig. 1C) and tracked BNF using acetylene reduction assays (ARAs) with a 2.5%
312 acetylene headspace concentration (see Material and Methods). This concentration of
313 acetylene decreased but did not prevent the growth of *Dv*H or *Cp* (Supplementary Figs. S3A
314 and S4A). BNF generally decreased within the 26 h after the addition of varying
315 concentrations of NH_4^+ (10 – 3,000 µM) (Fig. 1C). However, the response of *Dv*H BNF to
316 NH_4^+ addition was highly dependent on both the concentration of added NH_4^+ and the timing
317 of sampling after the addition, as has been found for the DIN sensitivity of other diazotrophs
318 (Drozd et al., 1972; Holl & Montoya, 2005).

319 To better understand the relative contributions of BNF and external NH_4^+ to fulfilling cellular
320 N growth demands, we calculated the contribution of BNF to new biomass production (Fig.
321 1D) using the quantity of newly fixed N (derived from ARA activity), the increase in biomass
322 (measured as OD_{600}), and the quantity of N required to produce 1 OD equivalent of biomass
323 under N_2-fixing and NH_4^+-utilizing conditions (Supplementary Methods S1). Figure 1C shows
324 the reliance on BNF to fulfill N demands depends on the amount of added NH_4^+ and that
325 higher initial spike concentrations result in longer times for the resumption of BNF. At the
326 highest NH_4^+ addition (3,000 µM), the contribution of BNF to cellular N supply dropped to 0
327 in less than six hours and never resumed, showing that the amount of added NH_4^+ was more
328 than sufficient for the culture to complete growth under our conditions. Lower concentrations
329 of added NH_4^+ (< 300 µM) led to an initial drop in BNF followed by a slow increase back to
330 ~100% of its contribution to N supply, indicating that cells fully assimilated the added NH_4^+ to
331 support their growth. At the first sampling time point (3 h), addition of NH_4^+ > 100 µM showed
332 similarly low residual contributions of BNF to growth (~10-15% of initial BNF activity, Fig. 1C
333 and D) implying that at these concentrations the time to the onset of BNF inhibition (T_R, *i.e.*

the time necessary for the cell to sense external NH_4^+, modify its metabolism, and significantly decrease BNF), is independent of NH_4^+ concentration. By extrapolating the contribution of BNF to the time space, and assuming a drastic shift from nitrogen fixation to NH_4^+ uptake at T_R, 100% BNF contribution continues for a maximum of 15% of 3 h = 30 min after addition, then drops to 0%. Hence, in liquid culture of *Dv*H, T_R < ~ 30 min. In the first 3 h, residual contributions of BNF to cell growth were higher for NH_4^+ additions < 100 µM than when > 100 µM was added (e.g., 50% at 30 µM vs. 15% at 100 µM), and we found no inhibition at the lowest level of added NH_4^+ (10 µM), suggesting that T_R might be concentration-dependent at low external NH_4^+ concentrations (10 - 30µM).

Ammonium sensitivity of BNF in batch cultures of sulfate-reducing and fermenting bacteria

To determine the ambient NH_4^+ concentrations associated with changes in BNF activity, we simultaneously measured BNF activity and medium [NH_4^+] in NH_4^+ addition experiments with *Dv*H, (Fig. 2A and Supplementary Fig. S3), *Cp* (Fig. 2B and Supplementary Fig. S4), and two sulfate-reducing microbial enrichment consortia SRBB1 and SRBB2 dominated by *Desulfovibrio desulfuricans* sp. (Fig. 2C and Supplementary Fig. S5). Biological N fixation rates in all culture incubations decreased after NH_4^+ was added to cultures growing in fully diazotrophic conditions (Fig. 2A-C, Supplementary Fig. S3-S5). We did not find any evidence of BNF activity in *Dv*H and SRBBs enrichment when measured ambient NH_4^+ concentrations were > 2 µM (Fig. 2A and C, Supplementary Fig. S3 and S5). Consistent with our previous experiments with *Dv*H (Fig. 1D), interpolations of BNF rates before and after NH_4^+ addition for *Dv*H, SRBB2, and *Cp* (dashed lines, Fig. 2A-C), showed noticeable inhibition of BNF in all cultures within 0.5 - 3 h post-addition. After ammonium addition, bacterial uptake of NH_4^+ for growth led to the removal of > 400 µM NH_4^+ in less than 30 h for *Dv*H (max uptake rate ~ 500 $\mu M_{NH4+}.OD^{-1}.h^{-1}$) and in less than 4 h for *Cp* (see Supplementary Figs. S3-S5). Full removal of NH_4^+ coincides with the recommencement of BNF (e.g., resumption of ethylene production in Fig. 2A-C).

Ammonium sensitivity of BNF in sulfate-reducing salt marsh sediments

To evaluate the sensitivity of BNF by benthic organisms to NH_4^+ under conditions that are more representative of natural environments, we performed incubation experiments on slurries of salt marsh sediments collected from Barnegat Bay (NJ), Sippewissett Bay (MA), and Great Bay (NH) (Fig. 2D-F, Supplementary Figs. S6 and S7). We evaluated BNF using both ARA and ^{15}N tracer methods to account for possible artifacts associated with the use of acetylene to estimate BNF (Fulweiler et al., 2015; Payne & Grant, 1982). For both ARA and $^{15}N_2$ tracer incubations (10 incubations per method), we observed the onset of BNF only after the levels of dissolved NH_4^+ initially present in slurries decreased drastically (to $[NH_4^+] <$ 20 µM) (Fig. 2D-F, Supplementary Figs. S6 and S7). In the $^{15}N_2$ tracer incubations, five of ten samples (Supplementary Fig. S7 #3, #5, #6, #7, and #9) showed a decrease in ^{15}N incorporation into organic matter before NH_4^+ addition, and two of them completely stopped incorporation of ^{15}N (Supplementary Fig. S7 #3 and #9). In parallel, NH_4^+ concentrations slightly increased from < 8 µM to levels around 10-18 µM in several samples prior to NH_4^+ addition (Supplementary Fig. S7 #3, #4, #5, and #9), suggesting the presence of some endogenic NH_4^+ production within our experiments.

Similar to our results with cultured diazotrophs, NH_4^+ additions (e.g., target $[NH_4^+] \sim 300$ µM, indicated with arrow, Fig. 2E and F) to actively fixing samples coincided with a fast decrease in ethylene production to a complete stop in less than ~ 3 h in all our samples (n=20). For four of the eight ARA-assayed sediment samples (two each from NH and MA salt marshes) spiked with NH_4^+, BNF responded normally to NH_4^+, *i.e.* BNF rates resumed to pre-addition values once ambient NH_4^+ was drawn down to near background levels ($[NH_4^+] <$ 10 µM, Fig. 2E, Supplementary Fig. S6), likely due to assimilatory or dissimilatory biological activities. The post-addition results from the other four of eight ARA samples with NH_4^+ added (two each from NH and MA salt marshes) were excluded because of dubious OPA measurements of $[NH_4^+]$ (see Methods and Supplementary Discussion). Importantly, none of the 10 sediment incubations assayed using the ^{15}N tracer method, which directly reflects

387 BNF activity, showed any evidence of a resumption of BNF activity after NH_4^+ addition, and
388 post-addition NH_4^+ concentrations never decreased below 50 µM (Fig. 2F and
389 Supplementary Fig. S7). We note that the general decrease in $\delta^{15}N$ of OM in these samples
390 after NH_4^+ addition is consistent with the assimilation of the unlabeled NH_4^+ added to the
391 incubation, which could also impact the timing and sensitivity of the method to detect BNF.

392 *Determination of NH_4^+ threshold for benthic BNF*

393 Fast removal of ammonium from media due to high metabolic activity (*e.g*., growth) of the
394 samples, uncertainties on the ethylene concentration in headspace due to sequential dilution
395 during sampling, and variations in the timing for the BNF inhibition response after NH_4^+
396 addition all preclude a direct measurement of the exact ammonium concentration at which
397 BNF stops. To obtain a best estimate of the threshold for ammonium inhibition of BNF for
398 each type of experiment, we used the 95th percentile of all measured NH_4^+ concentrations
399 where BNF was present (before NH_4^+ addition) or resumed (after NH_4^+ addition) as a robust
400 estimate for the threshold NH_4^+ concentration that induce changes in BNF activity (Fig. 3,
401 number of datapoints for cultures in liquid media: n=10, ARA sediment slurries: n=52, and
402 ^{15}N tracer sediment slurries: n=20). For each sample, significant BNF activity corresponds to
403 BNF activity > 5% of the maximal BNF activity. Results from *Cp* were not included in this
404 analysis as we could not verify the complete inhibition followed by resumption of BNF in any
405 of our replicates (Fig. 2B and Supplementary Fig. S4). This is likely due to the removal of
406 NH_4^+ faster being than the response time for complete BNF inhibition by the fast-growing *Cp*
407 cultures, as well as by our limited sampling frequency.

408 Threshold values of $[NH_4^+]$ are < 2 µM (average ± SD of 0.7 ± 0.7 µM) for all sulfate-
409 reducing liquid media cultures (*Dv*H and SRBB1 and SRBB2, Fig. 3A), consistent with
410 values obtained for other cultured diazotrophs (Dekaezemacker & Bonnet, 2011; Sweet &
411 Burris, 1981) and oligotrophic pelagic BNF (Knapp, 2012). We note that the actual threshold
412 value is likely lower than our reported estimate of 2 µM because of the precision of the NH_4^+

measurement in our conditions (reproducibility$_{0\text{-}10\mu M}$ ~ 1 µM). While the fast growth, fast removal of ammonium, and our insufficient sampling frequency does not allow for an accurate determination of NH_4^+ threshold in *Cp*, we estimate that its value to be anywhere between 0 and 20 µM, as evidenced by BNF slow-down ~3 h post-ammonium addition and its recommencement ~10 hr post-addition (Fig. 2B, ammonium at t~ 8h vs 14 hr). Threshold values of ~ 7 µM and ~ 11 µM were found for BNF in slurries assessed by ARA and ^{15}N tracer methods, respectively (Fig. 3B and C). This value is in good agreement with similar experiments performed with deep-sea sediments (< 25 µM) (Dekas et al., 2018). All these direct measurements of NH_4^+ thresholds are consistent with calculations of the external [NH_4^+] at which BNF resumes in experiments with *Dv*H (Fig. 1C and D) that account for the drawdown of external NH_4^+ contributing to biomass growth ([NH_4^+]$_{calculated}$ < 23 µM, Supplementary Methods S2 and Fig. S8).

Diazotrophic community in enrichment cultures and slurry experiments

In both SRBB1 and SRBB2, *nifH* taxonomic diversity was dominated by several operational taxonomic units (OTUs) closely related to the SRB *Desulfovibrio desulfuricans*. SRBB1 showed the additional presence of an OTU closely related to the genus *Clostridium* (Supplementary Fig. S1A). Other OTUs (e.g., *Desulfovibrio fructosovorans, Azotobacter vinelandii,* and *Pelobacter carbinolicus*) were found in low abundance (<1% of total *nifH genes).* The 16S rRNA gene diversity confirmed the dominance of *Desulfovibrio* and *Clostridium* species in the enrichments (Supplementary Fig. S1B).

To determine the diazotrophic community that developed in our sediment incubations and compare them to those in other benthic environments, we sequenced *nifH*, which encodes a component of the Mo-nitrogenase and is the most common phylogenetic marker used in studies of diazotroph diversity (Fig. 4). Analysis of *nifH* gene diversity in DNA extracted from sediments at the end of incubation (5 days) revealed the dominance of sequences related to those from delta-proteobacteria, particularly sulfate-reducing genera

(closely related to *Desulfovibrio desulfuricans, D. salexigens, Desulfatibacillum alkenivorans, Desulfuromonas acetoxidans*), as well as other anaerobic bacteria (*e.g*. *Pelobacter carbinolicus* and *Marichromatium purpuratum*). These diazotrophic taxa have also been identified in other salt marshes (Burns et al., 2002; Steppe & Paerl, 2005), and in estuarine (Burns et al., 2002; Newell, Pritchard, et al., 2016), and deep-sea sediments (Gier et al., 2016; Kapili et al., 2020). Examination of *nifH* transcript diversity at the end of incubations showed similar results suggesting that the putative diazotrophs identified based on *nifH* gene diversity are likely active during our incubation (Fig. 4A and Supplementary Fig. S9).

Relationship between nitrogenase activity and sediment biogeochemical characteristics

The richness of *nifH* transcripts (expressed as observed number of OTUs, Fig. 5A) was similar at the end of incubations, even in treatments exhibiting high final concentrations of NH_4^+ (> 100 µM) and no $^{15}N_2$ incorporation or acetylene reduction activity in the previous 20-30 h (Fig. 2, symbol gradient shade in Fig. 5A, Supplementary Fig. S6 and S7). Biological N fixation activity at the end of incubation was only detected for NH_4^+ concentrations less than ~ 20 µM. This strongly supports a post-transcriptional inhibition of nitrogenase activity by NH_4^+ and slow turnover of *nifH* transcripts in our incubations.

Hierarchical clustering of our samples and Canonical Analysis of Principal Coordinates on the OTU abundance data (Hellinger transformation) indicates that geographical origin (NJ, MA, and NH) rather than the type of incubation (*i.e*., BNF assayed by ARA or ^{15}N) best explains sediment *nifH* composition (see colored boxes in top panel Fig. 4B, Fig. 5B, and Supplementary Fig. S10). We identified several OTUs showing significant differences in relative abundance between ARA and ^{15}N incubation conditions based on 16S rRNA gene diversity, but not for *nifH* gene and transcript abundance (Supplementary Fig. S10C). Net NH_4^+ removal rates (as the balance between all processes that remove NH_4^+ minus the potential release of NH_4^+ from sediments) are correlated with initial (pre-addition) NH_4^+

concentrations, and maximum BNF rates are positively correlated with sediment C:N ratios (Fig. 5C).

Literature review of benthic porewater ammonium concentrations

To estimate the extent to which BNF can occur in benthic sediments (Fig. 6A), we combine all data by transforming the ARA- and ^{15}N-based results so that they are relative to the maximum in each replicate ($(V_{BNF,Max} - V_{BNF}) / V_{BNF,Max}$). It allows us to derive a single estimate of NH_4^+ threshold for BNF in sediments of $[NH_4^+]_{threshold}$ = 9 µM (Fig. 6B, n=72). We then analyzed porewater ammonium concentration data from 26 studies including 151 sites and more than 300 individual samples representing a diversity of benthic environments (Fig. 6C and D, SI Table S1). We estimate the fraction of global sediments where BNF might occur by deriving the depth ('threshold depth', see Fig. 6A) at which published porewater $[NH_4^+]$ equaled the threshold value of BNF inhibition of NH_4^+ = 9 µM (Fig. 6C and D). The median depth at which porewater ammonium reaches the threshold value is 0.3 cm (Fig. 6C, average 0.65 cm, range 0 – 25 cm, n=151). In this review, ~ 87 % of the values collected (based on individual cores, n=334) exceeded the $[NH_4^+]_{threshold}$ at depths deeper than 1 cm below surface, and 95 % of values exceeded the threshold at depths of ~ 3 cm below surface. Porewater $[NH_4^+]$ was lower than the threshold at any measured depth in only ~ 0.1% of all individual cores (3 of 334). Results separated along the different benthic zones, *i.e.*, tidal (< 4 m, n=64), sub-littoral (between 4 and 200 m, n=47), and bathyal (> 200 m, n=40), are available in Supplementary Fig. S12.

Discussion

Metabolic cost of BNF in anaerobic diazotrophs

The metabolic cost of using BNF versus fixed N sources like ammonium to support growth can yield insights on ecophysiologies of microorganisms in nature. The substantively lower

489 growth rates and yields observed for diazotrophic versus ammoniotrophic growth of the
490 sulfate-reducer *Dv*H (2-fold growth rate and yield) and the fermenter *Cp* (1.5-fold growth rate,
491 1.2-fold yield) indicate a significant metabolic cost of BNF as an N source in anaerobic
492 bacteria. The cost of BNF in diazotrophs that have metabolisms involving O_2 is even more
493 substantial given the additional energetic costs of protecting nitrogenase and other O_2-
494 sensitive BNF-related enzymes from oxidative damage (Großkopf & LaRoche, 2012;
495 Inomura et al., 2017) Collectively, the physiological data for anaerobic diazotrophs presented
496 here, as for other types of diazotrophs, support the paradigm of prevalent BNF in
497 environments with limiting amounts of fixed N.

498 *Ammonium threshold for BNF in diazotrophic bacteria and its relation to cellular N*
499 *metabolism*

500 Our results show that BNF activity in sulfate-reducing bacteria and sulfate-reducing
501 sediments is sensitive to fixed nitrogen (as NH_4^+) at micromolar concentrations. This
502 conclusion does not appear to support the use of BNF as an important mechanism to
503 balance intracellular redox in ammonium-rich benthic systems, as previously hypothesized
504 (Tichi & Tabita, 2000). The onset of inhibition of BNF activity occurs for $[NH_4^+]_{threshold} < 2$ µM
505 in liquid cultures of SRB; a slightly higher threshold of $[NH_4^+]_{threshold} < 11$ µM was found in
506 slurry incubations. This is in good agreement with existing knowledge of the biochemistry
507 and metabolism of nitrogen fixers (Dekaezemacker & Bonnet, 2011; Hartmann et al., 1986;
508 Holl & Montoya, 2005; Kleiner, 1974; Ohki et al., 1991; Postgate & Kent, 1984). Our
509 threshold estimates are also consistent with early studies in salt-marsh sediments
510 ($[NH_4^+]_{threshold} < 33$ µM) (Carpenter et al., 1978; Patriquin & Keddy, 1978), a recent studies of
511 BNF in deep-sea sediments ($[NH_4^+]_{threshold} < 25$ µM) (Dekas et al., 2018), and pure culture
512 studies with *Desulfovibrio gigas (*$[NH_4^+]_{threshold} \sim 10$ µM) (Kessler et al., 2001; Postgate &
513 Kent, 1984), *Rhodospirullum rubrum* ($NH_4^+]_{threshold} \sim 3$-5 µM) (Sweet & Burris, 1981),
514 *Klebsiella oxytoca* ($[NH_4^+]_{threshold} < 10$ µM) (Schreiber et al., 2016), *Methanoccocus*
515 *maripaludis* ($[NH_4^+]_{threshold} < 25$ µM) (Kessler et al., 2001), *Azotobacter vinelandii*

516 ($[NH_4^+]_{threshold}$ < 10 µM) (Kleiner, 1974), and *Trichodesmium* ($[NH_4^+]_{threshold}$ < 10 µM)
517 (Mulholland et al., 2001), and *Crocosphaera watsonii* ($[NH_4^+]_{threshold}$ < 1 µM)
518 (Dekaezemacker & Bonnet, 2011). While the ammonium threshold of BNF inhibition could
519 not be precisely estimated for the fermenter *Clostridium pasteurianum* ($[NH_4^+]_{threshold}$ < 20
520 µM) due to rapid ammonium draw-down and low sampling frequency, the presence of
521 *Clostridia* relatives in the isolate SRBB1 (Supplementary Figs. S1 and S4) and Clostridia-like
522 *nifH* sequences in sediment slurries suggest a similarly high sensitivity.

523 Biological N fixation and NH_4^+ uptake are complementary N sources to cells. Nitrogenase
524 activity and gene regulation is controlled by intracellular NH_4^+ through the GS-GOGAT
525 systems. In most diazotrophs, low NH_4^+ supply to the cell leads to a decrease in intracellular
526 glutamine concentrations, turning on nitrogenase gene transcription and/or nitrogenase
527 protein activity through the PII signal-transduction cascade (Dixon & Kahn, 2004).
528 Conversely, sufficient NH_4^+ supply to the cell decreases BNF, either at the pre- or post-
529 transcriptional level. Cellular N and C metabolisms are coupled via the balance between α-
530 ketoglutarate, a metabolite of the TCA cycle, and glutamine (Huergo & Dixon, 2015).
531 Extracellular N sources are acquired through the use of specific membrane transporters (e.g.,
532 AmtB for ammonium (Kleiner, 1985; Zheng et al., 2004)). Most other fixed-N sources, such
533 as NO_3^-, are first taken up and then intracellularly converted into ammonia by specific
534 enzymes (e.g., nitrate reductase) before being used anabolically. Assuming a Michaelis
535 Menten mechanism for NH_4^+ transport (Kuzyakov & Xu, 2013), we expect the affinity
536 constant of the NH_4^+ transporter to play a critical role in cellular sensing of and ability to grow
537 using external NH_4^+ (Javelle et al., 2004), thereby modulating internal N status and BNF
538 down-regulation (Fig. 6A). For example, at NH_4^+ concentrations < K_m of the transporter, less
539 than 50% of NH_4^+ uptake activity can take place, reducing intracellular N concentrations and
540 inducing a metabolic cascade that ultimately leads to the onset of BNF activity. This
541 simplified framework would constrain the switch between ammoniotrophy and BNF or their
542 co-occurrence to NH_4^+ concentrations close to transporter K_m values (Schreiber et al., 2016).

In reviewing the literature, we found that the K_m values for AmtB, the most common NH_4^+ transport protein, in a variety of nitrogen fixers, range in value from approximately 1 to 20 µM (Kleiner, 1985). These values are in good accordance with our experimental data and prior literature which show BNF inhibition thresholds of 2-10 µM NH_4^+. Given these estimates, BNF activity in environment with high N loadings would not be unexpected when residual dissolved NH_4^+ concentrations are < 20 µM (Foster & Fulweiler, 2014).

Timing of inhibition and regulation of nitrogenase in anaerobic diazotrophs

We found that T_R, the time to the onset of BNF inhibition after NH_4^+ addition, was concentration-independent at [NH_4^+] > 100 µM, and concentration-dependent at [NH_4^+] < 30 µM, in accordance with a Michaelis-Menten mechanism for NH_4^+ sensing. Within this framework, the lowest addition of NH_4^+ in this study (10 µM), which led to the longest delay (> 3 h) in BNF inhibition (see Fig. 1D), can be explained by a sub-maximal uptake of NH_4^+ leading to the delay in cellular metabolic response. The passive diffusion of ammonia through cell membranes is not likely to be important as the pH of media was ~ 7 and rate of removal was faster in the faster growing bacteria (i.e., *Cp*) than in *Dv*H, indicating an active process.

The relatively short-time response of BNF to NH_4^+ additions in both pure culture and slurry incubations (0.5 - 3h, as estimated from BNF rate interpolations, Fig. 2) and mass balance calculations in Fig. 1D) and the fast resumption of BNF activity upon depletion of the external NH_4^+ pool indicates that the control of NH_4^+ over nitrogenase activity is most likely post-transcriptional. This is also supported by the presence of multiple *nifH* mRNA from SRB clades within incubations with [NH_4^+] > 100 µM and no BNF activity. Boyd and co-workers have suggested that post-transcriptional regulation arose during the evolutionary transition from anaerobic to aerobic BNF as an early strategy of anaerobes for optimizing BNF activity in fluctuating environments (Boyd et al., 2015). Pure culture studies on anaerobic organisms (Heiniger & Harwood, 2015; Kessler et al., 2001; Masepohl et al., 2002) and field studies in

569 salt marsh sediments using methionine sulfoxide, an inhibitor of glutamine synthase, also
570 support this interpretation (Gandy & Yoch, 1988; Yoch & Whiting, 1986). The results of this
571 study, with frequent measurement of ammonium and BNF activity over the incubation period,
572 and the likely post-transcriptional nature of NH_4^+ inhibition of nitrogenase in anaerobic
573 systems, reiterates the need for higher time resolution flux measurements for better *in situ*
574 BNF estimates in natural environments.

575 Interestingly, there is a drastic difference between the long lag-phase (~ 20-50h) at the initial
576 onset of diazotrophy both in *Dv*H cultures (without initial NH_4^+ and during the transition
577 between ammoniotrophy and diazotrophy) and in slurry incubations, and the rather rapid
578 inhibition and resumption of BNF following NH_4^+ removal in actively fixing samples (< 3h)
579 (Fig. 1C and Fig. 2). This suggests that SRB organisms living in environments with
580 fluctuating N concentrations close to the NH_4^+ threshold value might maintain an intracellular
581 nitrogenase pool that can help them quickly resume BNF activity should there be local NH_4^+
582 depletion. Interestingly, BNF in *Cp* cultures remained active for ~ 3 hr after NH_4^+ addition
583 while NH_4^+ in media was quickly removed. Consistent with this observation, Yoch and
584 Whiting, 1986, found that undisturbed sediments amended with mannose, a preferred
585 substrate of fermenting bacteria, took longer to inhibit BNF than when lactate, a substrate
586 favoring SRBs, was used as the amended C source. In addition, and in opposition to our
587 findings with SRB, only scarce *nifH* transcripts attributed to *Clostridia* were found at the end
588 of our incubation experiments compared to their general presence in our samples (Fig. 4 and
589 Supplementary Fig. S10), indicating that transcriptional regulation of the *nif* genes could be
590 more prominent in this strain. The data suggest that even though the ammonium threshold
591 between SRB and firmicutes is likely similar, the sensing mechanism or inhibition pathway
592 could slightly differ (Gandy & Yoch, 1988; Gordon et al., 1981; Postgate & Kent, 1984; Tubb
593 & Postgate, 1973). How these differences in regulatory pathways influence the adaptation
594 and competitiveness of these organisms in benthic systems remains to be investigated.

595

Implications for benthic diazotrophy and the marine N budget

Consistent with previous studies of saltmarsh, estuarine, and carbonate mud sediments (reviewed by Capone, 1988; see also Welsh et al., 1996), we find strong and consistent inverse relationships between ambient ammonium and BNF activity. Our estimate of NH_4^+ threshold for BNF in sediments of $[NH_4^+]_{threshold}$ = 9 µM (Fig. 6B, n=72). This value is lower than any previously reported value for BNF inhibition in sediments, and is consistent with a very early assessment of *in-situ* BNF sensitivity to porewater NH_4^+ in *Spartina* marshes ($[NH_4^+]_{threshold}$ between 3 and 33 µM) (Patriquin & Keddy, 1978) and recent estimates in deep-sea sediments ($[NH_4^+]_{threshold}$< 25 µM) (Dekas et al., 2018).

The potential diazotrophic genera identified in our sediment slurry experiments overlap well with those found in other benthic systems, from intertidal salt marshes (Burns et al., 2002; Steppe & Paerl, 2005), and estuaries (0-20m water level) (Burns et al., 2002; Newell, Pritchard, et al., 2016) to deep oceanic floor sediment (100-1000m) (Gier et al., 2015; Kapili et al., 2020), with the dominance of *Desulfovibriaceae, Desulfobulbacee*, as well as some Firmicutes species (see Fig. 4). We found evidence in several of our samples for the presence and transcriptional activity of *Pelobacter carbolinicus* and *Desulfuromonas acetoxidans*, which have been identified in a recent study on the diazotrophic community of deep sea sediments using ^{15}N-SIP-RNA to probe the identity of the dominant diazotrophs (Kapili et al., 2020). The observation of similar microbiome composition indicates that our threshold estimates likely represent the general response of SRBs and possibly of other types of anaerobic N fixers present in benthic systems (*e.g.*, potential fermenters in SRBB1 diazotroph enrichment, Supplementary Fig. S1).

In situ porewater $[NH_4^+]$ in most benthic sediments (Knapp, 2012) is usually higher than our observed threshold (> 10-20 µM) and increases with depth (Metzger et al., 2019) (Fig. 6A). Our review of porewater ammonium data from 26 studies, including 151 sites and more than 300 individual samples indicates that the median depth at which our threshold value was

622 reached is 0.3 cm below sediment surface (Fig. 6C, based on site, average 0.65 cm, range 0
623 – 25cm, n=151). Overall, in our review, ~ 87% of the values collected (based on individual
624 cores, n=334) were over our $[NH_4^+]_{threshold}$ at a depth greater than 1 cm, and 95% at depth of
625 ~ 3 cm. This analysis suggests that BNF rates in sediments are likely to be greatest at the
626 surface and decrease rapidly to zero. Diffusion of O_2 from the sediment-water interface into
627 deeper layers could further reduce the opportunity for BNF to occur.

628 The previously reported relatively high ammonium values associated with BNF inhibition, like
629 those reviewed in Capone 1988 (~200-300 µM) and Knapp et al 2012 (50-2,000 µM), were
630 likely due to long incubation times (> 24 hr), the fast depletion of porewater ammonium, and
631 the reporting of *in situ* porewater $[NH_4^+]$ rather than measurement of ambient $[NH_4^+]$ during
632 incubation. Consistent with our results, many studies that track the timeline of N fixation
633 show very little if any activity in the first ~ 24 - 48 hr of incubation in saltmarsh sediments
634 when roots were excluded (Patriquin & Keddy, 1978; Yoch & Whiting, 1986). In contrast, *in*
635 *situ* incubations of vegetated saltmarshes sediments (Yoch & Whiting, 1986) demonstrate
636 rapid onset of BNF and the highest activity was found with surface-washed living roots and
637 rhizome samples, and with C addition, indicating a predominant role of root-associated
638 microbes and available C (*i.e*., carbon substrate amendment, root exudates).

639 Thus, our results, which are compatible with our knowledge of the regulation of diazotrophy
640 (Dixon & Kahn, 2004), suggest that the extent of natural BNF activity in benthic sediments
641 may be mostly limited to N-limited superficial regions of the sediments (top 1 cm, Fig. 6) and
642 highly productive environments like seagrass meadows and *Spartina* marshes. The
643 observation of BNF associated with live vegetation roots in *Spartina* marsh with high $[NH_4^+]$
644 (Yoch & Whiting, 1986) is likely explained by local zones around and within plant roots
645 (Kuzyakov & Xu, 2013) in which NH_4^+ is depleted by plant and microbial uptake to
646 concentrations below our threshold estimates.

Our findings do not contradict the traditional view of a relatively small contribution of benthic systems to total marine BNF compared to pelagic new N sources. Early studies have suggested benthic contributions to global marine BNF of ~ 15 Tg N (Capone, 1988; Capone & Carpenter, 1982), ~10% of total BNF (Zhang et al., 2020). Most of this activity was then attributed to shallow benthic environments, particularly vegetated and coral reef ecosystems. Based on the recent findings of Dekas et *al*. 2017 and consistent with our analyses of ammonium thresholds (Supplementary Fig.S12), it is possible that unvegetated sediments from the deep sea could constitute a larger source of new N than previously thought. More precise accounting of benthic BNF however requires additional measurements in these and other benthic systems that account for several methodological challenges in measuring BNF, which we discuss below.

Current methodologies for BNF investigations in sediments

Our results show that the timing of inhibition is a critical factor to consider when assessing the sensitivity of BNF to ammonium as a fixed N source. Measurement of BNF activity before the onset of the inhibition response would lead to the false conclusion that BNF in a tested sample is not or little sensitive to ammonium. Conversely, it is particularly critical to measure and report the evolution of [NH_4^+] over time along or at the end of incubations, as typical incubation times, which range from 8 hours to several days, are sufficient for pore water [NH_4^+] > 100 µM to become depleted to background NH_4^+ levels (below threshold for BNF activation). This precaution is particularly important in closed and semi-closed vessel experiments with high activity samples (e.g., experiments with carbon addition, high C:N sediments, and pure cultures), where ammonium-supported growth would drastically increase the biomass and lead to higher BNF rates after fixed N addition.

Our measurements show that the apparent NH_4^+ concentration required to stop BNF in slurry experiments ([NH_4^+] < 11 µM, Fig. 3B and C) is roughly five times higher than in liquid media

673 experiments (*Dv*H and SRBB enrichments, [NH_4^+] < 2 µM, Fig. 3A). It is probable that our
674 measurement of the NH_4^+ concentration threshold for BNF is higher in the sediment slurries
675 due to higher spatial and temporal heterogeneity. Small biogeochemically distinct zones, or
676 microniches, could originate from slow nutrient diffusion to hotspots of highly active biomass
677 in heterogenous sediments and lead to imbalanced macronutrient ratios (C or P excess
678 relative to N). Indeed, our results show an association between maximal BNF rate and high
679 C:N (Fig. 5C), and reports on the occurrence of BNF at high fixed N have been correlated
680 with high C:N ratios of sediments (Hou et al., 2018). We particularly expect microniche
681 formation to be favored at high cell densities when the requirement for N in a large
682 population of active cells could outpace the diffusion of porewater NH_4^+ through the solid
683 phase. These conditions would prevail at the end of our incubations (~4-5 d) when the
684 addition of NH_4^+ and of 30 mM lactate, a readily available source of carbon to SRBs, resulted
685 in a high density of biomass. In addition, the heterogeneity of organic matter in our samples
686 is suggested by the high variability of sample C and N composition (Table 1), and even
687 though agitation was constant during our experiment, we observed macroscopic clumping of
688 slurry material and vegetation debris throughout the incubation period. The threshold NH_4^+
689 concentration values reported here were obtained for a wide range of sediment chemical
690 and isotopic composition (*i.e.*, %C, %N, C:N, δ13C, and δ15N, see Table 1), suggesting that
691 our threshold value should be general and apply to many benthic environments.

692 It is important to note both here and in other studies, the presence of *nifH* genes and
693 transcripts do not provide definitive proof of BNF activity in anaerobic settings, as we found
694 evidence consistent with post-transcriptional BNF regulation in benthic SRBs. In addition,
695 prolonged incubation (5 days for ARA or $^{15}N_2$ uptake experiments) along with addition of
696 carbon and sulfur (lactate + sulfate) could have drastically altered the biogeochemical
697 conditions within our microcosms (buildup of H_2S, removal of nutrients) and selected for
698 diazotroph species different from those important in natural microbial assemblages. These
699 long incubation periods could also have led to other artifacts that directly interfered with our

700 study, such as the rapid drawdown of high *in situ* NH_4^+ and abnormal NH_4^+ measurements
701 with the OPA method (see Methods and Supplementary Fig. S2 and Supplementary
702 Discussion), which strongly affect interpretations on the sensitivity of BNF activity to NH_4^+
703 (Supplementary Fig. S6 #4, #6, #9 & #10). In this regards, the use of *in situ* measurements
704 (Yoch & Whiting, 1986) and of several existing (ARA, ^{15}N, MIMS) and newly developed
705 methodological approaches (Aoki & McGlathery, 2019) could help produce a more accurate
706 view of N cycling in sediments.

707 The use of high concentration of acetylene (~25% v/v) has been shown to influence the
708 microbiome (*16S* mRNA) of estuary sediment samples during short-term incubations (~ 7 h)
709 (Fulweiler et al., 2015). Indeed, we were able to identify changes in microbial composition
710 based on 16S rRNA genes at 2.5% acetylene over 5 days of incubation (Supplementary Fig.
711 S10C). However, there was no significant differences in the *nif*H gene or transcript diversity
712 (Fig. 5B and Supplementary Fig. S10A and B) or in the response of BNF to NH_4^+ addition
713 between ARA and $^{15}N_2$ tracer incubations (Fig. 3), indicating that the use of a sub-saturating
714 concentration of acetylene (2.5%v/v) did not interfere with our study. Indeed, estimates of
715 *Dv*H growth inhibition under these low acetylene conditions (μ_{C2H2} = 0.01 h-1 vs μ_{ctrl} = 0.016
716 h-1, 30-40% inhibition, Supplementary Fig. S3) is consistent with the flux of electron diverted
717 from N_2 reduction to produce ethylene during ARA, as evaluated by nitrogenase acetylene
718 saturation in the presence of dinitrogen(K_{mC2H2} ~ 0.5-4 kPa, ~40-60% saturation) (Davis &
719 Wang, 1980). This is in agreement with a previous report of acetylene inhibition in sulfate-
720 reducing bacteria (Payne & Grant, 1982), where an acetylene concentration of 5-10% only
721 partially inhibited growth rate and yield. In addition, the presence and activity of
722 molybdenum-independent nitrogenases in sediment (McRose et al., 2017; Zhang et al.,
723 2016) could also influence BNF rate determinations and the overall N input budget in benthic
724 areas when the ARA method is used without ^{15}N calibration (Bellenger et al., 2020). Indeed,
725 in our experiments, the average R ratio (i.e., C_2H_2 : N_2 ratio of activity), calculated with the
726 highest BNF rate reached for each method was 2.3 (range 0.16 – 5.5, n=10), possibly

indicative of the presence of alternative nitrogenase. Finally, in a set of unsuccessful experiments containing fresh salt marsh sediment from Barnegat Bay (n=6), overlying water, and addition of lactate, we did not observe any BNF activity (as AR and ^{15}N incorporation) over the course of one week and one month, respectively, even though *nifH* genes were presumably present in these sediments before our incubation (Fig. 4B). These results indicate that other factors, such as water quality, (micro-) nutrient availability, and the nature of the dissolved organic matter also likely influence the *in-situ* activity.

Conclusion

In this study, we demonstrate that various sulfate-reducing bacteria, and very likely fermenting clostridia, found in coastal sediments exhibit high sensitivity to NH_4^+ addition, with a [NH_4^+] threshold for BNF inhibition below 10 µM. To mechanistically link BNF inhibition and external NH_4^+ concentrations, we propose a simple framework of cellular N metabolism based on the affinity constant of the NH_4^+ transporter. The measured threshold is likely to apply to several benthic systems as the different diazotrophic genera identified here are similar to those described in sediments ranging from the deep sea to coasts. Analysis of published porewater data suggests that the vast majority of [NH_4^+] reported for sediments sampled at 1 cm below the sediment water interface exceed the threshold for BNF inhibition. The data are consistent with the existing framework for a relatively small contribution of benthic systems to marine new N inputs. Apparent discrepancies between our results and previous reports of low NH_4^+ sensitivity in benthic environments could be explained by porewater NH_4^+ concentrations close to the threshold value, fast removal of porewater NH_4^+, sediment heterogeneity, and by considering the timing necessary after addition of NH_4^+ for inhibition to be recorded (*e.g.* 30 min – 3 h as found here). Our research provides new mechanistic insights on the biogeochemistry of nitrogen input into marine ecosystems that can help improve N cycling models and guide future measurement studies of benthic BNF.

Acknowledgements

This research was funded by grants from the Simons Foundation (award ID 622944 to X.Z.), the Carbon Mitigation Initiative at Princeton University (to X.Z.), and a Simons Foundation / Life Science Research Foundation Postdoctoral Fellowship (to R.D). We thank the Barnegat Bay Foundation for aid in collecting salt marsh sediments, J. Wilmoth, C. Rusley, E. Zimble, and A. Jayakumar for aid with molecular analyses, the laboratories of B.W.Ward and D. Sigman for aid with DIN analyses, and members of the Zhang laboratory for useful discussions. Katja Luxem is on the Science Advisory Committee for the Watershed Institute (NJ, https://thewatershed.org/). The authors declare no other competing interests.

Availability statement

All the data used for this study are currently available in Supplementary Materials (Supplementary Materials _Dataset). Upon manuscript acceptance, the dataset files will be deposited to Figshare, all molecular datasets will be deposited on NCBI database, and the R Markdown code and associated files to reproduce all figures will be deposited at GitHub.

References:

Anderson, M. J., & Willis, T. J. (2003). Canonical analysis of principal coordinates: A useful method of constrained ordination for ecology. *Ecology*, *84*(2), 511–525. https://doi.org/10.1890/0012-9658(2003)084[0511:CAOPCA]2.0.CO;2

Aoki, L. R., & McGlathery, K. J. (2019). High rate of N fixation in seagrass sediment measured via a direct 30N2 push-pull method. *Marine Ecology Progress Series*, *616*, 1–11. https://doi.org/10.3354/meps12961

Bellenger, J.-P., Wichard, T., Xu, Y., & Kraepiel, A. M. L. (2011). Essential metals for nitrogen fixation in a free-living N2-fixing bacterium: chelation, homeostasis and high use efficiency. *Environmental Microbiology*, *13*(6), 1395–411. https://doi.org/10.1111/j.1462-2920.2011.02440.x

778 Bellenger, J.-P., Darnajoux, R., Zhang, X., & Kraepiel, A. M. L. (2020). Biological nitrogen
779 fixation by alternative nitrogenases in terrestrial ecosystems: a review. *Biogeochemistry*,
780 *149*(1), 53–73. https://doi.org/10.1007/s10533-020-00666-7

781 Bertics, V. J., Sohm, J. A., Treude, T., Chow, C. E. T., Capone, D. G., Fuhrman, J. A., &
782 Ziebis, W. (2010). Burrowing deeper into benthic nitrogen cycling: The impact of
783 Bioturbation on nitrogen fixation coupled to sulfate reduction. *Marine Ecology Progress*
784 *Series*, *409*, 1–15. https://doi.org/10.3354/meps08639

785 Bertics, V. J., Löscher, C. R., Salonen, I., Dale, A. W., Gier, J., Schmitz, R. A., & Treude, T.
786 (2013). Occurrence of benthic microbial nitrogen fixation coupled to sulfate reduction in
787 the seasonally hypoxic Eckernförde Bay, Baltic Sea. *Biogeosciences*, *10*(3), 1243–1258.
788 https://doi.org/10.5194/bg-10-1243-2013

789 van den Boogaart, K. G., & Tolosana-Delgado, R. (2008). “compositions”: A unified R
790 package to analyze compositional data. *Computers and Geosciences*, *34*(4), 320–338.
791 https://doi.org/10.1016/j.cageo.2006.11.017

792 Boyd, E. S., Garcia Costas, A. M., Hamilton, T. L., Mus, F., & Peters, J. W. (2015). Evolution
793 of molybdenum nitrogenase during the transition from anaerobic to aerobic metabolism.
794 *Journal of Bacteriology*, *197*(9), 1690–1699. https://doi.org/10.1128/JB.02611-14

795 Brown, S. M., & Jenkins, B. D. (2014). Profiling gene expression to distinguish the likely
796 active diazotrophs from a sea of genetic potential in marine sediments. *Environmental*
797 *Microbiology*, *16*(10), 3128–3142. https://doi.org/10.1111/1462-2920.12403

798 Burns, J. A., Zehr, J. P., & Capone, D. G. (2002). Nitrogen-fixing phylotypes of Chesapeake
799 Bay and neuse river estuary sediments. *Microbial Ecology*, *44*(4), 336–343.
800 https://doi.org/10.1007/s00248-002-1000-9

801 Capone, D. G. (1988). Benthic nitrogen fixation. In T. H. Blackburn & J. Sorensen (Eds.),

Nitrogen cycling in coastal marine environments (Vol. 139, pp. 498–499). John Wiley & Sons, Ltd. https://doi.org/10.1016/0769-2609(88)90114-7

Capone, D. G., & Carpenter, E. J. (1982). Nitrogen fixation in the marine environment. *Science*, *217*(4565), 1140–1142. https://doi.org/10.1126/science.217.4565.1140

Caporaso, J. G., Lauber, C. L., Walters, W. A., Berg-Lyons, D., Huntley, J., Fierer, N., et al. (2012). Ultra-high-throughput microbial community analysis on the Illumina HiSeq and MiSeq platforms. *The ISME Journal 2012 6:8*, *6*(8), 1621–1624. https://doi.org/10.1038/ismej.2012.8

Carpenter, E. J., Van Raalte, C. D., & Valiela, I. (1978). Nitrogen fixation by algae in a Massachusetts salt marsh. *Limnology and Oceanography*, *23*(2), 318–327. https://doi.org/10.4319/lo.1978.23.2.0318

Codispoti, L. A. (2007). An oceanic fixed nitrogen sink exceeding 400 Tg N a-1 vs the concept of homeostasis in the fixed-nitrogen inventory. *Biogeosciences*, *4*(2), 233–253. https://doi.org/10.5194/bg-4-233-2007

Davis, L. C., & Wang, Y. L. (1980). In vivo and in vitro kinetics of nitrogenase. *Journal of Bacteriology*, *141*(3), 1230–1238. https://doi.org/10.1128/jb.141.3.1230-1238.1980

Dekaezemacker, J., & Bonnet, S. (2011). Sensitivity of N2 fixation to combined nitrogen forms (NO3- and NH4+) in two strains of the marine diazotroph Crocosphaera watsonii (Cyanobacteria). *Marine Ecology Progress Series*, *438*, 33–46. https://doi.org/10.3354/meps09297

Dekas, A. E., Fike, D. A., Chadwick, G. L., Green-Saxena, A., Fortney, J., Connon, S. A., et al. (2018). Widespread nitrogen fixation in sediments from diverse deep-sea sites of elevated carbon loading. *Environmental Microbiology*, *20*(12), 4281–4296. https://doi.org/10.1111/1462-2920.14342

826 Dixon, R., & Kahn, D. (2004). Genetic regulation of biological nitrogen fixation. *Nature*
827 *Reviews. Microbiology*, *2*(8), 621–631. https://doi.org/10.1038/nrmicro954

828 Drozd, J. W., Tubb, R. S., & Postgate, J. R. (1972). A chemostat study of the effect of fixed
829 nitrogen sources on nitrogen fixation, membranes and free amino acids in Azotobacter
830 chroococcum. *Journal of General Microbiology*, *73*(2), 221–232.
831 https://doi.org/10.1099/00221287-73-2-221

832 Elser, J. J., Bracken, M. E. S., Cleland, E. E., Gruner, D. S., Harpole, W. S., Hillebrand, H.,
833 et al. (2007). Global analysis of nitrogen and phosphorus limitation of primary producers
834 in freshwater, marine and terrestrial ecosystems. *Ecology Letters*, *10*(12), 1135–1142.
835 https://doi.org/10.1111/j.1461-0248.2007.01113.x

836 Foster, S. Q., & Fulweiler, R. W. (2014). Spatial and historic variability of benthic nitrogen
837 cycling in an anthropogenically impacted estuary. *Frontiers in Marine Science*, *1*(NOV),
838 56. https://doi.org/10.3389/fmars.2014.00056

839 Fulweiler, R. W., Nixon, S. W., Buckley, B. A., & Granger, S. L. (2007). Reversal of the net
840 dinitrogen gas flux in coastal marine sediments. *Nature*, *448*(7150), 180–182.
841 https://doi.org/10.1038/nature05963

842 Fulweiler, R. W., Heiss, E. M., Rogener, M. K., Newell, S. E., LeCleir, G. R., Kortebein, S. M.,
843 & Wilhelm, S. W. (2015). Examining the impact of acetylene on N-fixation and the active
844 sediment microbial community. *Frontiers in Microbiology*, *6*(MAY).
845 https://doi.org/10.3389/fmicb.2015.00418

846 Gandy, E. L., & Yoch, D. C. (1988). Relationship between nitrogen-fixing sulfate reducers
847 and fermenters in salt marsh sediments and roots of Spar. *Applied and Environmental*
848 *Microbiology*, *54*(8), 2031–2036. https://doi.org/10.1128/aem.54.8.2031-2036.1988

849 Gier, J., Sommer, S., Löscher, C. R., Dale, A. W., Schmitz, R. A., & Treude, T. (2015).

Nitrogen fixation in sediments along a depth transect through the Peruvian oxygen minimum zone. *Biogeosciences Discussions*, *12*(17), 14401–14440. https://doi.org/10.5194/bgd-12-14401-2015

Gier, J., Sommer, S., Löscher, C. R., Dale, A. W., Schmitz, R. A., & Treude, T. (2016). Nitrogen fixation in sediments along a depth transect through the Peruvian oxygen minimum zone. *Biogeosciences*, *13*(14), 4065–4080. https://doi.org/10.5194/bg-13-4065-2016

Glibert, P. M., Wilkerson, F. P., Dugdale, R. C., Raven, J. A., Dupont, C. L., Leavitt, P. R., et al. (2016). Pluses and minuses of ammonium and nitrate uptake and assimilation by phytoplankton and implications for productivity and community composition, with emphasis on nitrogen-enriched conditions. *Limnology and Oceanography*, *61*(1), 165–197. https://doi.org/10.1002/lno.10203

Gloor, G. B., Macklaim, J. M., Pawlowsky-Glahn, V., & Egozcue, J. J. (2017, November 15). Microbiome datasets are compositional: And this is not optional. *Frontiers in Microbiology*. Frontiers Media S.A. https://doi.org/10.3389/fmicb.2017.02224

Gordon, J. K., Shah, V. K., & Brill, W. J. (1981). Feedback inhibition of nitrogenase. *Journal of Bacteriology*, *148*(3), 884–888. https://doi.org/10.1128/jb.148.3.884-888.1981

Goto, M., Ando, S., Hachisuka, Y., & Yoneyama, T. (2005). Contamination of diverse *nifH* and *nifH* -like DNA into commercial PCR primers. *FEMS Microbiology Letters*, *246*(1), 33–38. https://doi.org/10.1016/j.femsle.2005.03.042

Großkopf, T., & LaRoche, J. (2012). Direct and indirect costs of dinitrogen fixation in Crocosphaera watsonii WH8501 and possible implications for the nitrogen cycle. *Frontiers in Microbiology*, *3*(JUL). https://doi.org/10.3389/fmicb.2012.00236

Gruber, N., & Galloway, J. N. (2008, January 17). An Earth-system perspective of the global

nitrogen cycle. *Nature*. Nature Publishing Group. https://doi.org/10.1038/nature06592

Hardy, R. W. F., Holsten, R. D., Jackson, E. K., & Burns, R. C. (1968). The acetylene - ethylene assay for N2 fixation : laboratory and field evaluation. *Plant Physiology*, *43*(1968), 1185–1207.

Hartmann, A., Fu, H., & Burris, R. H. (1986). *Regulation of nitrogenase activity by ammonium chloride in Azospirillum spp*. *Journal of Bacteriology*.

Heidelberg, J. F., Seshadri, R., Haveman, S. A., Hemme, C. L., Paulsen, I. T., Kolonay, J. F., et al. (2004). The genome sequence of the anaerobic, sulfate-reducing bacterium Desulfovibrio vulgaris Hildenborough. *Nature Biotechnology*, *22*(5), 554–559. https://doi.org/10.1038/nbt959

Heiniger, E. K., & Harwood, C. S. (2015). Posttranslational modification of a vanadium nitrogenase. *MicrobiologyOpen*, *4*(4), 597–603. https://doi.org/10.1002/mbo3.265

Holl, C. M., & Montoya, J. P. (2005). Interactions between nitrate uptake and nitrogen fixation in continuous cultures of the marine diazotroph Trichodesmium (Cyanobacteria). *Journal of Phycology*, *41*(6), 1178–1183. https://doi.org/10.1111/j.1529-8817.2005.00146.x

Holmes, R. M., Aminot, A., Kérouel, R., Hooker, B. A., & Peterson, B. J. (1999). A simple and precise method for measuring ammonium in marine and freshwater ecosystems. *Canadian Journal of Fisheries and Aquatic Sciences*, *56*(10), 1801–1808. https://doi.org/10.1139/f99-128

Hou, L., Wang, R., Yin, G., Liu, M., & Zheng, Y. (2018). Nitrogen fixation in the intertidal sediments of the Yangtze estuary: Occurrence and environmental implications. *Journal of Geophysical Research: Biogeosciences*, *123*(3), 936–944. https://doi.org/10.1002/2018JG004418

898 Huergo, L. F., & Dixon, R. (2015). The emergence of 2-oxoglutarate as a master regulator
899 metabolite. *Microbiology and Molecular Biology Reviews*, *79*(4), 419–435.
900 https://doi.org/10.1128/mmbr.00038-15

901 Inomura, K., Bragg, J., & Follows, M. J. (2017). A quantitative analysis of the direct and
902 indirect costs of nitrogen fixation: A model based on Azotobacter vinelandii. *ISME*
903 *Journal*, *11*(1), 166–175. https://doi.org/10.1038/ismej.2016.97

904 Javelle, A., Severi, E., Thornton, J., & Merrick, M. (2004). Ammonium sensing in Escherichia
905 coli: Role of the ammonium transporter Amtb and AmtB-GlnK complex formation.
906 *Journal of Biological Chemistry*, *279*(10), 8530–8538.
907 https://doi.org/10.1074/jbc.M312399200

908 Jayakumar, A., Chang, B. X., Widner, B., Bernhardt, P., Mulholland, M. R., & Ward, B. B.
909 (2017). Biological nitrogen fixation in the oxygen-minimum region of the eastern tropical
910 North Pacific ocean. *ISME Journal*, *11*(10), 2356–2367.
911 https://doi.org/10.1038/ismej.2017.97

912 Kapili, B. J., Barnett, S. E., Buckley, D. H., & Dekas, A. E. (2020). Evidence for
913 phylogenetically and catabolically diverse active diazotrophs in deep-sea sediment.
914 *ISME Journal*, *14*(4), 971–983. https://doi.org/10.1038/s41396-019-0584-8

915 Kessler, P. S., Daniel, C., & Leigh, J. A. (2001). Ammonia switch-off of nitrogen fixation in
916 the methanogenic archaeon Methanococcus maripaludis: Mechanistic features and
917 requirement for the novel GlnB homologues, NifI1 and NifI2. *Journal of Bacteriology*,
918 *183*(3), 882–889. https://doi.org/10.1128/JB.183.3.882-889.2001

919 Kleiner, D. (1974). Quantitative relations for the repression of nitrogenase synthesis in
920 Azotobacter vinelandii by ammonia. *Archives of Microbiology*, *101*(1), 153–159.
921 https://doi.org/10.1007/BF00455935

922 Kleiner, D. (1985). Bacterial ammonium transport. *FEMS Microbiology Letters*, *32*(2), 87–
923 100. https://doi.org/10.1016/0378-1097(85)90059-X

924 Knapp, A. N. (2012). The sensitivity of marine N2 fixation to dissolved inorganic nitrogen.
925 *Frontiers in Microbiology*, *3*(OCT), 374. https://doi.org/10.3389/fmicb.2012.00374

926 Kuzyakov, Y., & Xu, X. (2013). Competition between roots and microorganisms for nitrogen:
927 Mechanisms and ecological relevance. *New Phytologist*, *198*(3), 656–669.
928 https://doi.org/10.1111/nph.12235

929 Lespinat, P. A., Berlier, Y. M., Fauque, G. D., Toci, R., Denariaz, G., & LeGall, J. (1987). The
930 relationship between hydrogen metabolism, sulfate reduction and nitrogen fixation in
931 sulfate reducers. *Journal of Industrial Microbiology*, *1*(6), 383–388.
932 https://doi.org/10.1007/BF01569336

933 Masepohl, B., Drepper, T., Paschen, A., Gross, S., Pawlowski, A., Raabe, K., et al. (2002).
934 Regulation of nitrogen fixation in the phototrophic purple bacterium Rhodobacter
935 capsulatus. *Journal of Molecular Microbiology and Biotechnology*, *4*(3), 243–8.

936 McMurdie, P. J., & Holmes, S. (2013). Phyloseq: An R package for reproducible interactive
937 analysis and graphics of microbiome census data. *PLoS ONE*, *8*(4).
938 https://doi.org/10.1371/journal.pone.0061217

939 McRose, D. L., Zhang, X., Kraepiel, A. M. L., & Morel, F. M. M. (2017). Diversity and activity
940 of alternative nitrogenases in sequenced genomes and coastal environments. *Frontiers*
941 *in Microbiology*, *8*, 267. https://doi.org/10.3389/fmicb.2017.00267

942 Metzger, E., Barbe, A., Cesbron, F., Thibault de Chanvalon, A., Jauffrais, T., Jézéquel, D., &
943 Mouret, A. (2019). Two-dimensional ammonium distribution in sediment pore waters
944 using a new colorimetric diffusive equilibration in thin-film technique. *Water Research X*,
945 *2*, 100023. https://doi.org/10.1016/j.wroa.2018.100023

946 Mohr, W., Großkopf, T., Wallace, D. W. R., & LaRoche, J. (2010). Methodological
947 underestimation of oceanic nitrogen fixation rates. *PLoS ONE*, *5*(9), 1–7.
948 https://doi.org/10.1371/journal.pone.0012583

949 Montoya, J. P., Voss, M., Kähler, P., & Capone, D. G. (1996). A simple , high-precision ,
950 high-sensitivity tracer assay for N2 fixation. *Applied and Environmental Microbiology*,
951 *62*(3), 986–993.

952 Mulholland, M. R., Ohki, K., & Capone, D. G. (2001). Nutrient controls on nitrogen uptake
953 and metabolism by natural populations and cultures of Trichodesmium (Cyanobacteria).
954 *Journal of Phycology*, *37*(6), 1001–1009. https://doi.org/10.1046/j.1529-
955 8817.2001.00080.x

956 Newell, S. E., Pritchard, K. R., Foster, S. Q., & Fulweiler, R. W. (2016). Molecular evidence
957 for sediment nitrogen fixation in a temperate New England estuary. *PeerJ*, *2016*(1),
958 e1615. https://doi.org/10.7717/peerj.1615

959 Newell, S. E., McCarthy, M. J., Gardner, W. S., & Fulweiler, R. W. (2016). Sediment nitrogen
960 fixation: a call for re-evaluating coastal N budgets. *Estuaries and Coasts*, *39*(6), 1626–
961 1638. https://doi.org/10.1007/s12237-016-0116-y

962 Ohki, K., Zehr, J. P., Falkowski, P. G., & Fujita, Y. (1991). Regulation of nitrogen-fixation by
963 different nitrogen sources in the marine non-heterocystous cyanobacterium
964 Trichodesmium sp. NIBB1067. *Archives of Microbiology*, *156*(5), 335–337.
965 https://doi.org/10.1007/BF00248706

966 Oksanen, J. F., Blanchet, G., Friendly, M., Kindt, R., Legendre, P., & McGlinn, D. (2019).
967 vegan: Community Ecology Package.

968 Patriquin, D. G., & Keddy, C. (1978). Nitrogenase activity (acetylene reduction) in a Nova
969 Scotian salt marsh: Its association with angiosperms and the influence of some edaphic

970 factors. *Aquatic Botany*, *4*(C), 227–244. https://doi.org/10.1016/0304-3770(78)90021-9

971 Payne, W. J., & Grant, M. A. (1982). Influence of acetylene on growth of sulfate-respiring
972 bacteria. *Applied and Environmental Microbiology*, *43*(3), 727–30.
973 https://doi.org/10.1128/AEM.43.3.727-730.1982

974 Postgate, J. R., & Kent, H. M. (1984). *Derepression of nitrogen fixation in Desulfovibrio gigas*
975 *and its stability to ammonia or oxygen stress in vivo*. *Journal of general microbiology*
976 (Vol. 130).

977 Price, M. N., Dehal, P. S., & Arkin, A. P. (2010). FastTree 2 - Approximately maximum-
978 likelihood trees for large alignments. *PLoS ONE*, *5*(3), e9490.
979 https://doi.org/10.1371/journal.pone.0009490

980 Riederer-Henderson, M. A., & Wilson, P. W. (1970). Nitrogen fixation by sulphate-reducing
981 bacteria. *Journal of General Microbiology*, *61*(1), 27–31.
982 https://doi.org/10.1099/00221287-61-1-27

983 Schreiber, F., Littmann, S., Lavik, G., Escrig, S., Meibom, A., Kuypers, M. M. M., &
984 Ackermann, M. (2016). Phenotypic heterogeneity driven by nutrient limitation promotes
985 growth in fluctuating environments. *Nature Microbiology*, *1*(6), 1–7.
986 https://doi.org/10.1038/nmicrobiol.2016.55

987 Sim, M. S., Wang, D. T., Zane, G. M., Wall, J. D., Bosak, T., & Ono, S. (2013). Fractionation
988 of sulfur isotopes by Desulfovibrio vulgaris mutants lacking hydrogenases or type I
989 tetraheme cytochrome c3. *Frontiers in Microbiology*, *4*(JUN).
990 https://doi.org/10.3389/fmicb.2013.00171

991 Sohm, J. A., Webb, E. A., & Capone, D. G. (2011). Emerging patterns of marine nitrogen
992 fixation. *Nature Reviews Microbiology*, *9*(7), 499–508.
993 https://doi.org/10.1038/nrmicro2594

994 Steppe, T. F., & Paerl, H. W. (2005). Nitrogenase activity and nifH expression in a marine
995 intertidal microbial mat. *Microbial Ecology*, *49*(2), 315–324.
996 https://doi.org/10.1007/s00248-004-0245-x

997 Sweet, W. J., & Burris, R. H. (1981). Inhibition of nitrogenase activity by NH4+ in
998 Rhodospirillum rubrum. *Journal of Bacteriology*, *145*(2), 824–831.
999 https://doi.org/10.1128/jb.145.2.824-831.1981

1000 Tichi, M. A., & Tabita, F. R. (2000). Maintenance and control of redox poise in Rhodobacter
1001 capsulatus strains deficient in the Calvin-Benson-Bassham pathway. *Archives of*
1002 *Microbiology*, *174*(5), 322–333. https://doi.org/10.1007/s002030000209

1003 Tubb, R. S., & Postgate, J. R. (1973). Control of nitrogenase synthesis in Klebsiella
1004 pneumoniae. *Journal of General Microbiology*, *79*(1), 103–117.
1005 https://doi.org/10.1099/00221287-79-1-103

1006 Voss, M., Bange, H. W., Dippner, J. W., Middelburg, J. J., Montoya, J. P., & Ward, B. (2013).
1007 The marine nitrogen cycle: Recent discoveries, uncertaintiesand the potential relevance
1008 of climate change. *Philosophical Transactions of the Royal Society B: Biological*
1009 *Sciences*, *368*(1621). https://doi.org/10.1098/rstb.2013.0121

1010 Welsh, D. T., Bourgués, S., De Wit, R., & Herbert, R. A. (1996). Seasonal variations in
1011 nitrogen-fixation (acetylene reduction) and sulphate-reduction rates in the rhizosphere
1012 of Zostera noltii: Nitrogen fixation by sulphate-reducing bacteria. *Marine Biology*, *125*(4),
1013 619–628. https://doi.org/10.1007/BF00349243

1014 Welsh, David T. (2000, January 1). Nitrogen fixation in seagrass meadows: Regulation,
1015 plant-bacteria interactions and significance to primary productivity. *Ecology Letters*.
1016 John Wiley & Sons, Ltd. https://doi.org/10.1046/j.1461-0248.2000.00111.x

1017 Westlake, D. W., & Wilson, P. W. (1959). Molecular hydrogen and nitrogen fixation by

1018 Clostridium pasteurianum. *Canadian Journal of Microbiology*, *5*, 617–620.
1019 https://doi.org/10.1139/m59-075

1020 Winogradsky, M. S. (1895). Sur l'assimilation de l'azote libre de l'atmosphere par les
1021 microbes. *Arch. Sci. Biol. St. Petersb.*, (3), 297–352.

1022 Yoch, D. C., & Whiting, G. J. (1986). Evidence for NH4+ switch-off regulation of nitrogenase
1023 activity by bacteria in salt marsh sediments and roots of the grass Spartina alterniflora.
1024 *Applied and Environmental Microbiology*, *51*(1), 143–149.
1025 https://doi.org/10.1128/aem.51.1.143-149.1986

1026 Zehr, J. P., & Kudela, R. M. (2011). Nitrogen cycle of the open ocean: From genes to
1027 ecosystems. *Annual Review of Marine Science*, *3*, 197–225.
1028 https://doi.org/10.1146/annurev-marine-120709-142819

1029 Zehr, J. P., & McReynolds, L. A. (1989). Use of degenerate oligonucleotides for amplification
1030 of the nifH gene from the marine cyanobacterium Trichodesmium thiebautii. *Applied*
1031 *and Environmental Microbiology*, *55*(10), 2522–2526.
1032 https://doi.org/10.1128/aem.55.10.2522-2526.1989

1033 Zehr, J. P., Mellon, M. T., & Zani, S. (1998). New nitrogen-fixing microorganisms detected in
1034 oligotrophic oceans by amplification of nitrogenase (nifH) genes. *Applied and*
1035 *Environmental Microbiology*, *64*(9), 3444–3450. https://doi.org/10.1128/aem.64.9.3444-
1036 3450.1998

1037 Zehr, J. P., Jenkins, B. D., Short, S. M., & Steward, G. F. (2003). Nitrogenase gene diversity
1038 and microbial community structure: A cross-system comparison. *Environmental*
1039 *Microbiology*, *5*(7), 539–554. https://doi.org/10.1046/j.1462-2920.2003.00451.x

1040 Zhang, X., McRose, D. L., Darnajoux, R., Bellenger, J.-P., Morel, F. M. M. M., & Kraepiel, A.
1041 M. L. L. (2016). Alternative nitrogenase activity in the environment and nitrogen cycle

implications. *Biogeochemistry*, *127*(2–3), 189–198. https://doi.org/10.1007/s10533-016-0188-6

Zhang, X., Ward, B. B., & Sigman, D. M. (2020, June 24). Global nitrogen cycle: critical enzymes, organisms, and processes for nitrogen budgets and dynamics. *Chemical Reviews*. American Chemical Society. https://doi.org/10.1021/acs.chemrev.9b00613

Zheng, L., Kostrewa, D., Bernèche, S., Winkler, F. K., & Li, X. D. (2004). The mechanism of ammonia transport based on the crystal structure of AmtB of Escherichia coli. *Proceedings of the National Academy of Sciences of the United States of America*, *101*(49), 17090–17095. https://doi.org/10.1073/pnas.0406475101

Figure Caption:

Figure 1: Effect of ammonium on growth and biological nitrogen fixation (BNF) in *Desulfovibrio vulgaris* var. Hildenborough (*Dv*H, Panels A, C and D) and *Clostridium pasteurianum* (*Cp*, Panel B). (A) Representative growth curves of *Dv*H for initial [NH_4^+] at the background concentration in diazotrophic media (< 10 µM), 500 µM, and 3,000 µM. Growth was supported by 30 mM pyruvate and sulfate. Error bars are standard deviations from one experiment (n=3). Growth rates are calculated from independent replicates (n=3) (B) Representative growth curves of *Cp* for initial [NH_4^+] at the background concentration in diazotrophic media (< 10 µM), 500 µM, and 3,000 µM. Growth was supported by fermentation of sucrose. Error bars are standard deviations from one experiment (n=3). Growth rates are calculated from independent replicates (n=3)(C) Relative BNF activity of *Dv*H was measured as the Acetylene Reduction Rate at 3h, 6h and 26h after addition of NH_4^+ (to concentrations of 10, 30, 100, 300, and 3,000 µM) compared to BNF activity before addition to *Dv*H grown under N_2-fixing conditions. Symbols represent individual samples

from a single experiment. (D) Estimated contribution of BNF to total N supply after ammonium additions. Error bars represent standard errors of the mean.

Figure 2: Effect of ammonium concentration on biological nitrogen fixation (BNF) activity in incubations of sulfate-reducing and fermenting microbes in culture and in sediments. (A-C) Medium [NH_4^+] (blue circles) and BNF activity (as accumulation of headspace ethylene, green squares for NH_4^+-amended) before and after addition of NH_4^+ to nitrogen limited, diazotrophic cultures of *Desulfovibrio vulgaris* var. Hildenborough (*Dv*H) (A), *Clostridium pasteurianum* (*Cp*) (B), and Barnegat Bay salt marsh enrichment strain SRBB2 (C) at OD ~ 0.1 (Supplementary Figs. S3-S5). Open symbols show BNF as ethylene (square) and dissolved [NH_4^+] (circle) in control experiments without addition of NH_4^+. (C-E) Dissolved [NH_4^+] (blue circles) and N_2 fixed equivalent (green squares, headspace ethylene for ARA and ^{15}N enrichment of particulate organic matter for ^{15}N tracer) over time in salt marsh sediment slurry incubations using ARA (C-D) and ^{15}N tracer methods (E). Additions are indicated with arrows. Only one representative replicate is shown to illustrate results for reasons of clarity. All incubation data (*Desulfovibrio vulgaris* n=6, SRBB1 n=2, SRBB2 n=2, salt marsh slurry n=10 for each method) are found in Supplementary Figures S3-S6 and summarized in Figure 3. Dashed lines illustrate interpolation of the BNF rate before and after NH_4^+ addition to estimate T_R, the time from ammonium addition to BNF inhibition.

Figure 2: Effect of ammonium concentration on biological nitrogen fixation (BNF) activity in incubations of sulfate-reducing microbes in culture and in sediments. (A and B) Medium [NH_4^+] (blue circles) and BNF activity (as accumulation of headspace ethylene, green squares for NH_4^+-amended) before and after addition of NH_4^+ to nitrogen limited, diazotrophic cultures of *Desulfovibrio vulgaris* var. Hildenborough (*Dv*H) (A) and Barnegat Bay salt marsh enrichment strain SRBB2 at OD_{600} ~ 0.1 (Supplementary Fig. S3 and S4). Open square symbols show control experiments without addition of ammonium. (C and D) Dissolved [NH_4^+] (blue circles) and N_2 fixed equivalent (green squares, headspace ethylene for ARA and ^{15}N enrichment of particulate organic matter for ^{15}N tracer) over time in

salt marsh sediment slurry incubations using ARA (C) and ^{15}N tracer methods (D). Additions are indicated with arrows. Only one representative replicate is shown to illustrate results for reasons of clarity. All incubation data (*Desulfovibrio vulgaris* n=6, SRBB1 n=2, SRBB2 n=2, salt marsh slurry n=10 for each method) are found in Supplementary Figures S3-S6 and summarized in Figure 3. Dashed lines illustrate interpolation of the BNF rate before and after NH_4^+ addition to estimate T_R, the time from ammonium addition to BNF inhibition.

Figure 3: Determination of threshold ammonium concentration (95th percentile) for inhibition of biological nitrogen fixation (BNF) in liquid cultures and sediment slurries. Combined results from incubations of *Desulfovibrio vulgaris* var. Hildenborough and SRBB1&2 consortia enriched from NJ salt marshes (A), ARA (B), and ^{15}N tracer (C) slurry incubations. BNF rates are the slope between time points from Figure 2. Blue boxes indicate the range of ammonium concentrations at which BNF was detected; black lines indicate average ammonium concentration, and dotted lines the 95-percentile (*i.e*. threshold values). The symbols distinguish data for BNF onset before (closed symbols) and BNF resumption after (open symbols) NH_4^+ addition. Panel C shows no post-addition data as BNF activity never resumed in ^{15}N tracer incubations of sediment (See Supplementary Fig. S6 and Fig. 2D). In panel B, post addition data for the 4 of 10 ARA incubations showing abnormal OPA measurements (See Supplementary Discussion) were highlighted with red stars.

Figure 4: Microbial composition of diazotroph community in salt marsh sediment incubations. (A) Phylogeny of the top 500 *nifH* genes OTUs (n=497) and the most abundant *nifH* trancripts OTUs (n=55, relative abundance>0.2%, total count >1000) from salt marsh slurry incubations relative to a representative subset (n=152) of a recently curated *nifH* library (Kapilli et *al.* 2020). Information on *nifH* genes for *Desulfovibrio vulgaris* v. Hildenborough (*Dv*H), and SRBB1 and SRBB2 enrichments consortia (n=46) are also shown. (B) Heatmap of *nifH* genes OTU relative abundance (log-scale) at the end of incubation with class-level information for the 500 first OTUs (bottom bar plot, > 80 % total abundance) and detailed phylogeny and closest relatives for the most abundant sequences (left panel, OTUs

with relative abundance >0.2% & total count >1000, n=59). Hierarchical clustering of individual sediment samples based on *nifH* composition (top left of panel) shows the relationship between sample *nifH* genes composition, incubation condition (ARA vs. ^{15}N), and geographical origin of the sediments. Purple box highlights low DNA samples with *nifH* composition similar to that of control extraction samples (reagent blank). Initial condition represents the samples before incubation.

Figure 5: Relationships between nitrogenase activity, microbial diversity, and sediment biogeochemical characteristics in sediment incubation. (A) Changes in richness (number of unique OTUs) in nitrogen fixer *nifH* transcripts at the end of incubation as a function of final ammonium concentrations (n=10). Symbol shade is proportional to the final BNF activity. (B) Discrimination analysis of nitrogen fixer communities (CAP analysis on Bray-Curtis distance). (C) Discriminant analysis of sediment biogeochemical activity and characteristics (redundancy analysis). In B and C, samples using acetylene reduction assay and ^{15}N tracer are highlighted in blue and green, respectively (shaded ovals represent 95% confidence ellipses) and axes show the percent of variance explained and the statistical significance for each explanatory axis as estimated using permutation Anova. Variables Bold are statistically significant in the model. In panel B, results were unchanged when we control for the origin of the sediment (NJ, NH, and MA).

Figure 6: Theoretical model for ammonium threshold for biological nitrogen fixation in benthic environments. (A) Overview of the Michaelis-Menten framework for NH_4^+ sensitivity applied to N-fixers in benthic environment, showing the effect of increasing pore water ammonium with depth on the transition from diazotrophy to ammoniotrophy. (B) Compilation of experimental data of model sulfate reducers *D. vulgaris H*. (ARA, N = 6 + 3 controls), SRBB enrichments (ARA, N = 4 + 2 controls), and three salt marshes of the Northeastern US (both ARA and ^{15}N, N=20) for $[NH_4^+] < 100$ µM. The red dashed vertical

line shows the 95-percentile [NH_4^+] (*i.e*. threshold value), and the dashed horizontal line indicated where BNF is 95% inhibited by ambient ammonium. (C) Frequency distribution of threshold depth (i.e., depth at which $[NH_4^+]_{threshold}$ was reached) derived from literature review of 26 study in several benthic environments (151 sites, 334 replicates, Supplementary Fig. S12 and Table S1). The red line represents cumulative frequencies, and the dashed vertical line represent the median value. (D) Geographic location and threshold depth (color scale) of reviewed study sites separate by benthic area (shape). Replicate numbers are proportional to point size.

Figure 1.

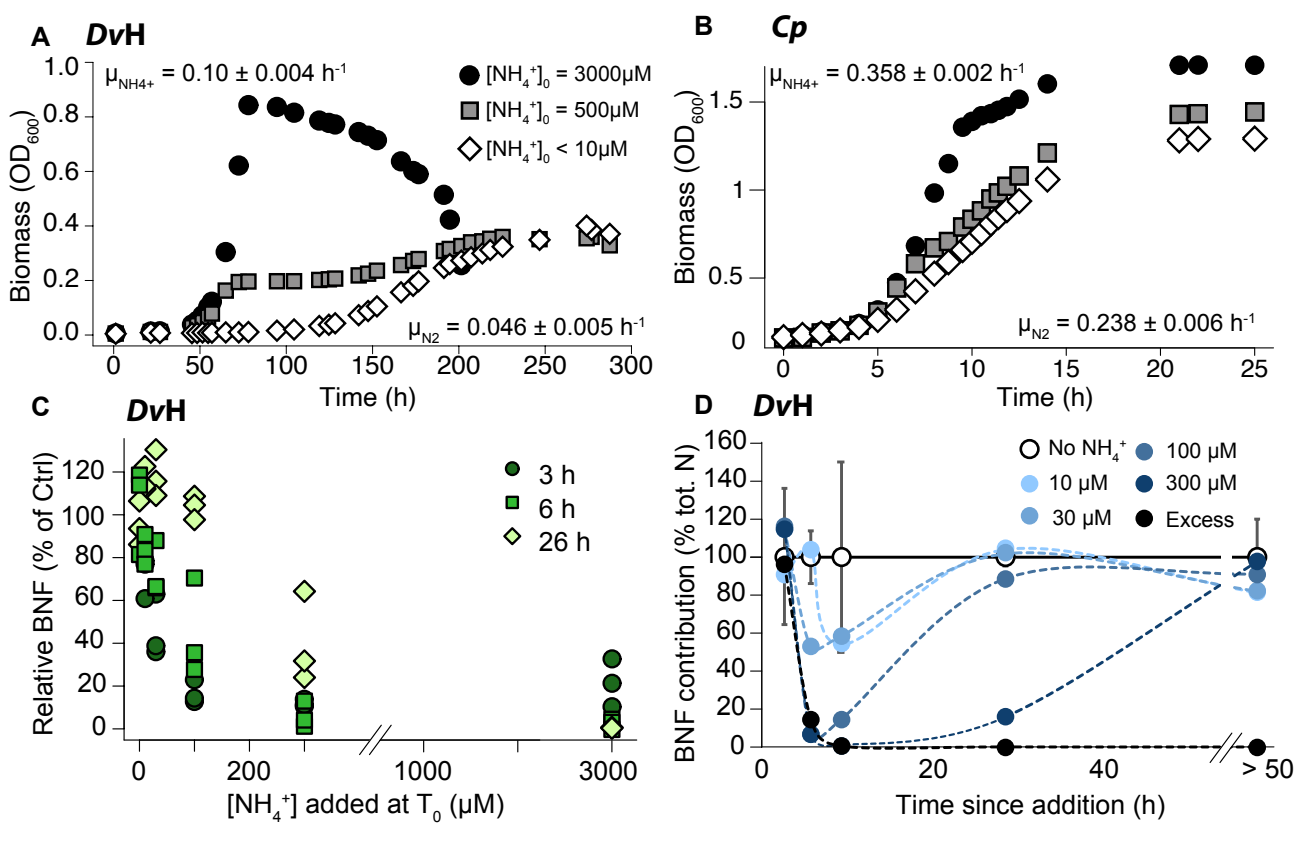
A
DvH
μNH4+ = 0.10 ± 0.004 h-1
[NH4+]0 = 3000μM
[NH4+]0 = 500μM
[NH4+]0 < 10μM
μN2 = 0.046 ± 0.005 h-1
Biomass (OD600)
Time (h)
B
Cp
μNH4+ = 0.358 ± 0.002 h-1
μN2 = 0.238 ± 0.006 h-1
Biomass (OD600)
Time (h)
C
DvH
Relative BNF (% of Ctrl)
3 h
6 h
26 h
[NH4+] added at T0 (μM)
D
DvH
No NH4+
10 μM
30 μM
100 μM
300 μM
Excess
BNF contribution (% tot. N)
Time since addition (h)

Figure 2.

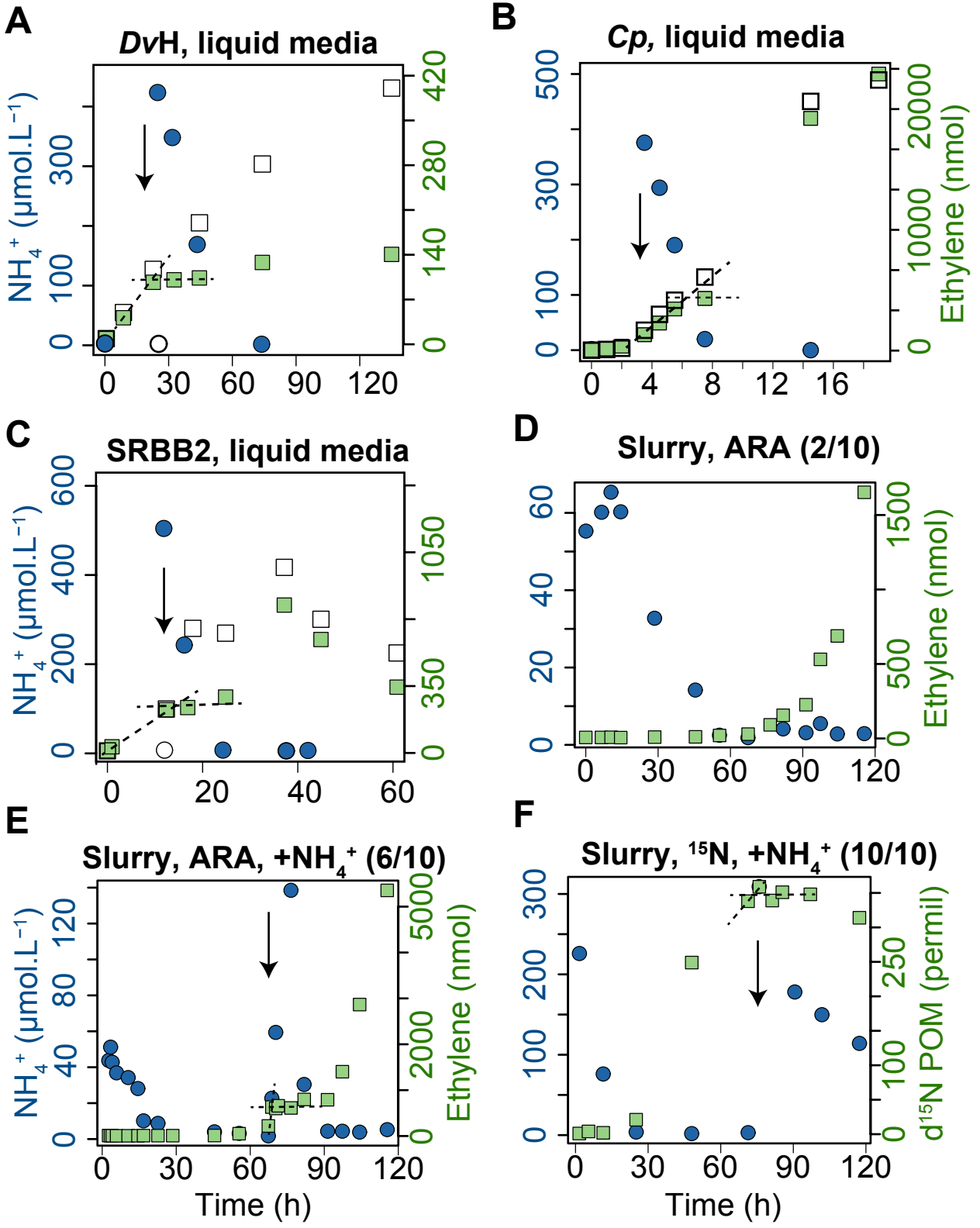
A
DvH, liquid media
B
Cp, liquid media
C
SRBB2, liquid media
D
Slurry, ARA (2/10)
E
Slurry, ARA, +NH4+ (6/10)
F
Slurry, 15N, +NH4+ (10/10)
NH4+ (µmol.L−1)
Ethylene (nmol)
d15N POM (permil)
Time (h)
[NH4+]
N-fixed eq.
[NH4+], control
N-fixed eq., control

Figure 3.

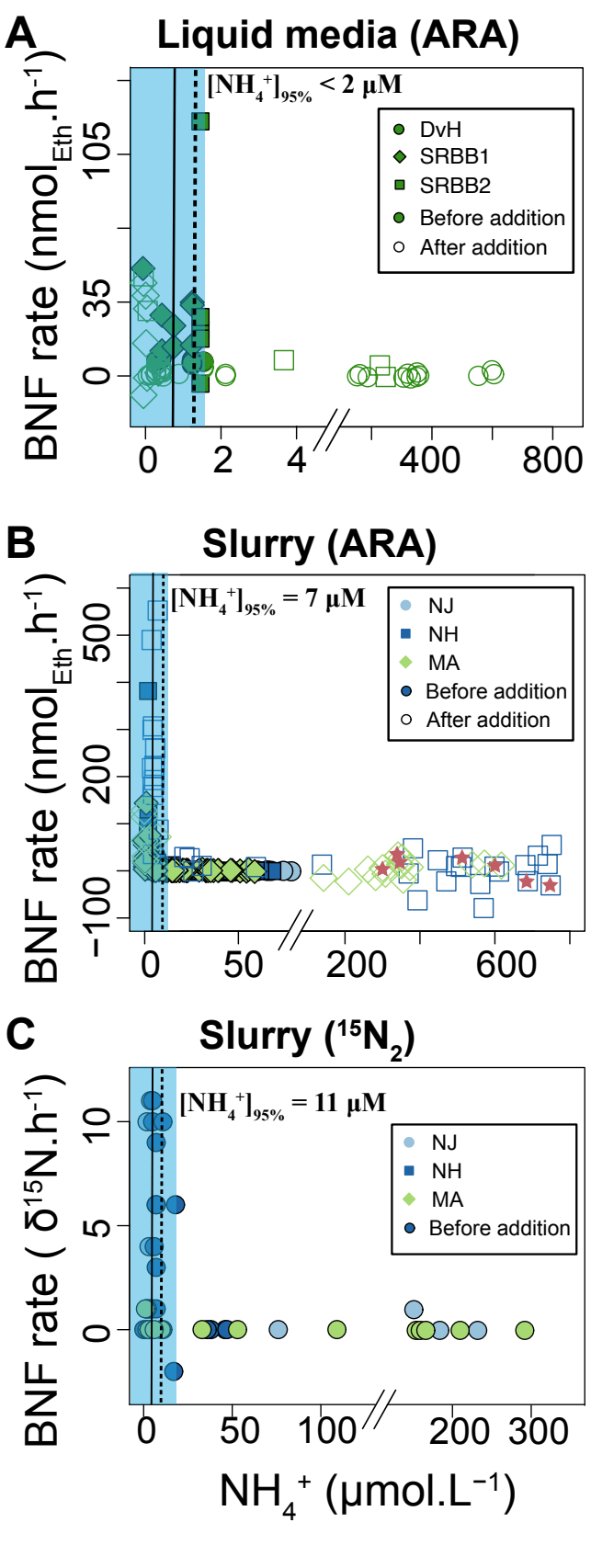
A
Liquid media (ARA)
BNF rate (nmol$_{Eth}$.h^{-1})
[NH$_4^+$]$_{95\%}$ < 2 µM
DvH
SRBB1
SRBB2
Before addition
After addition
105
35
0
0
2
4
400
800
B
Slurry (ARA)
BNF rate (nmol$_{Eth}$.h^{-1})
[NH$_4^+$]$_{95\%}$ = 7 µM
NJ
NH
MA
Before addition
After addition
500
200
−100
0
50
200
600
C
Slurry ($^{15}N_2$)
BNF rate (δ^{15}N.h^{-1})
[NH$_4^+$]$_{95\%}$ = 11 µM
NJ
NH
MA
Before addition
10
5
0
0
50
100
200
300
NH$_4^+$ (µmol.L^{-1})

Figure 4.

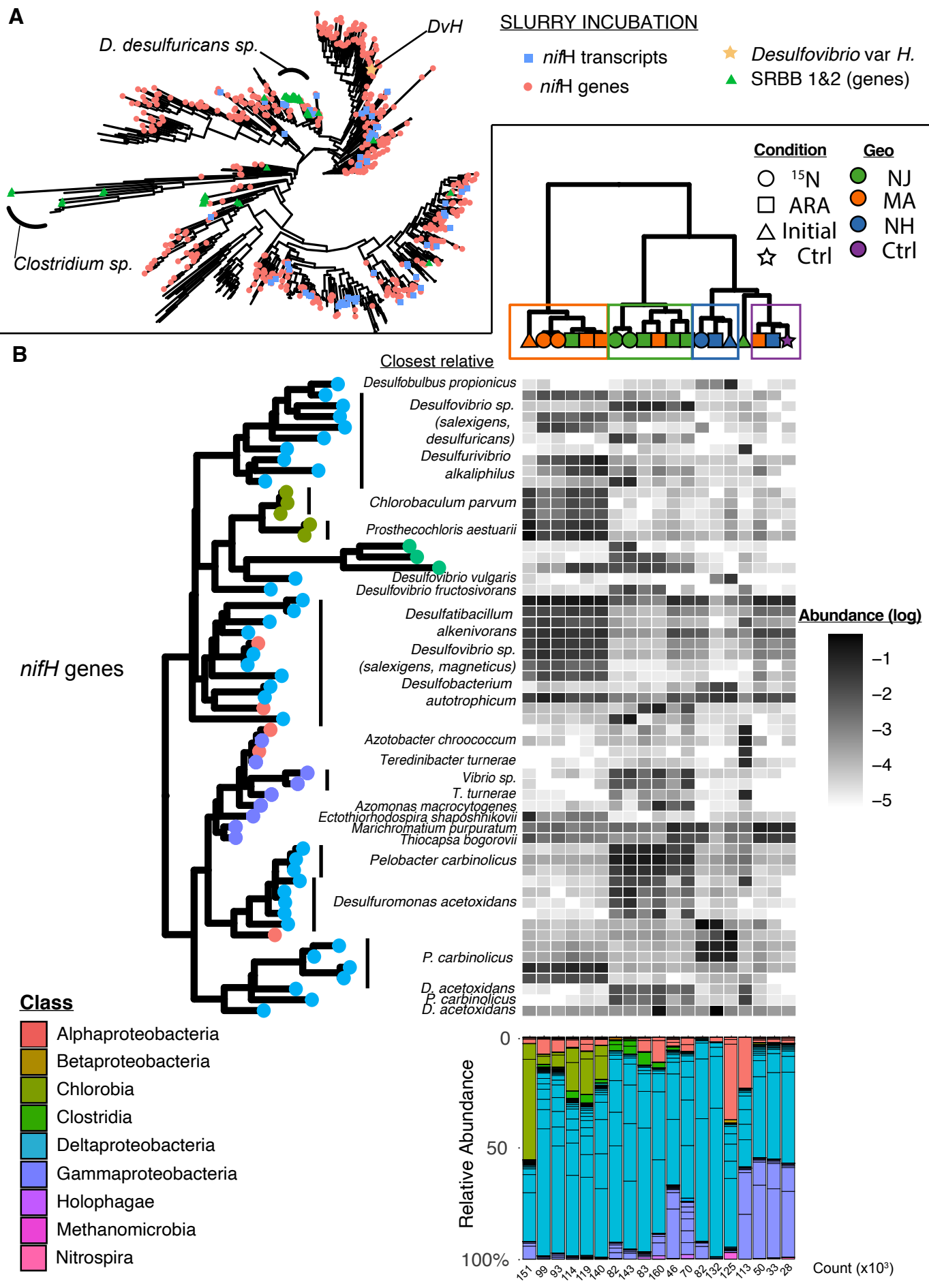
A
D. desulfuricans sp.
DvH
Clostridium sp.
SLURRY INCUBATION
nifH transcripts
nifH genes
Desulfovibrio var H.
SRBB 1&2 (genes)
Condition
15N
ARA
Initial
Ctrl
Geo
NJ
MA
NH
Ctrl
B
Closest relative
Desulfobulbus propionicus
Desulfovibrio sp. (salexigens, desulfuricans)
Desulfurivibrio alkaliphilus
Chlorobaculum parvum
Prosthecochloris aestuarii
Desulfovibrio vulgaris
Desulfovibrio fructosivorans
Desulfatibacillum alkenivorans
Desulfovibrio sp. (salexigens, magneticus)
Desulfobacterium autotrophicum
Azotobacter chroococcum
Teredinibacter turnerae
Vibrio sp.
T. turnerae
Azomonas macrocytogenes
Ectothiorhodospira shaposhnikovii
Marichromatium purpuratum
Thiocapsa bogorovii
Pelobacter carbinolicus
Desulfuromonas acetoxidans
P. carbinolicus
D. acetoxidans
P. carbinolicus
D. acetoxidans
nifH genes
Abundance (log)
−1
−2
−3
−4
−5
Class
Alphaproteobacteria
Betaproteobacteria
Chlorobia
Clostridia
Deltaproteobacteria
Gammaproteobacteria
Holophagae
Methanomicrobia
Nitrospira
Relative Abundance
0
50
100%
151 99 93 114 119 140 82 143 83 160 46 70 82 132 125 113 50 33 28
Count (x10³)

Figure 5.

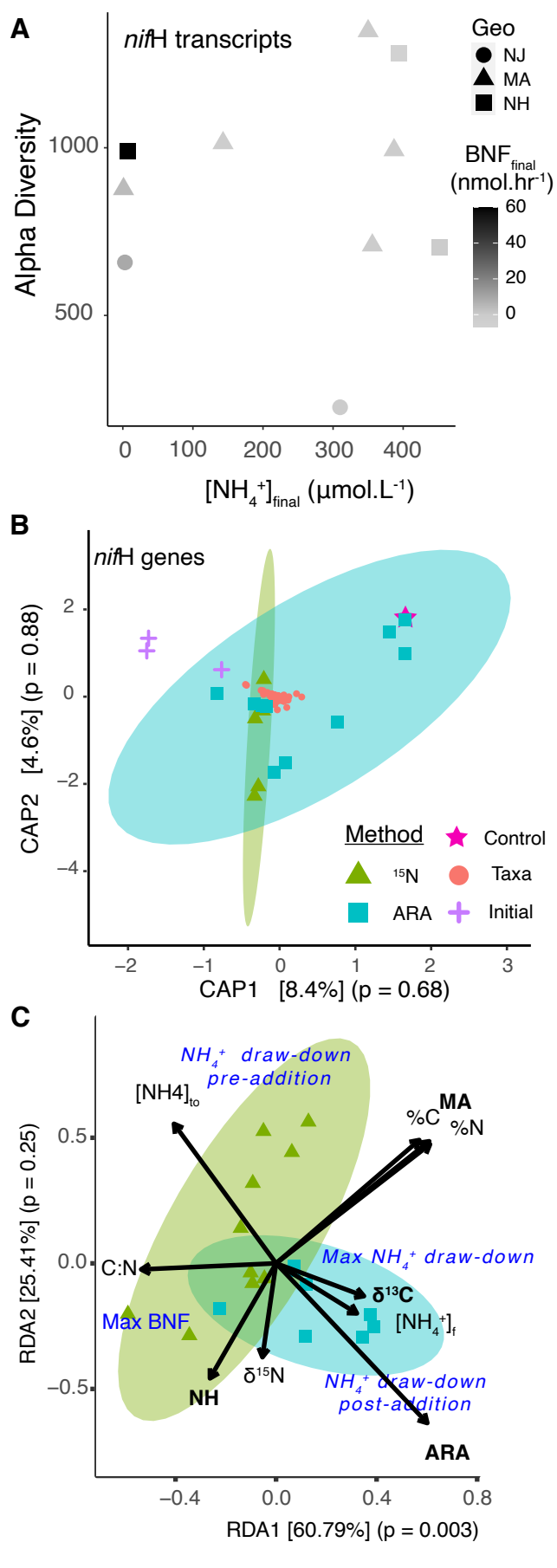
A
nifH transcripts
Geo
NJ
MA
NH
BNF final (nmol.hr-1)
60
40
20
0
Alpha Diversity
1000
500
0
100
200
300
400
[NH4+]final (µmol.L-1)
B
nifH genes
CAP2 [4.6%] (p = 0.88)
2
0
−2
−4
Method
Control
15N
Taxa
ARA
Initial
−2
−1
0
1
2
3
CAP1 [8.4%] (p = 0.68)
C
NH4+ draw-down pre-addition
[NH4]to
MA
%C
%N
0.5
0.0
−0.5
C:N
Max NH4+ draw-down
δ13C
Max BNF
[NH4+]f
δ15N
NH
NH4+ draw-down post-addition
ARA
RDA2 [25.41%] (p = 0.25)
−0.4
0.0
0.4
0.8
RDA1 [60.79%] (p = 0.003)

Figure 6.

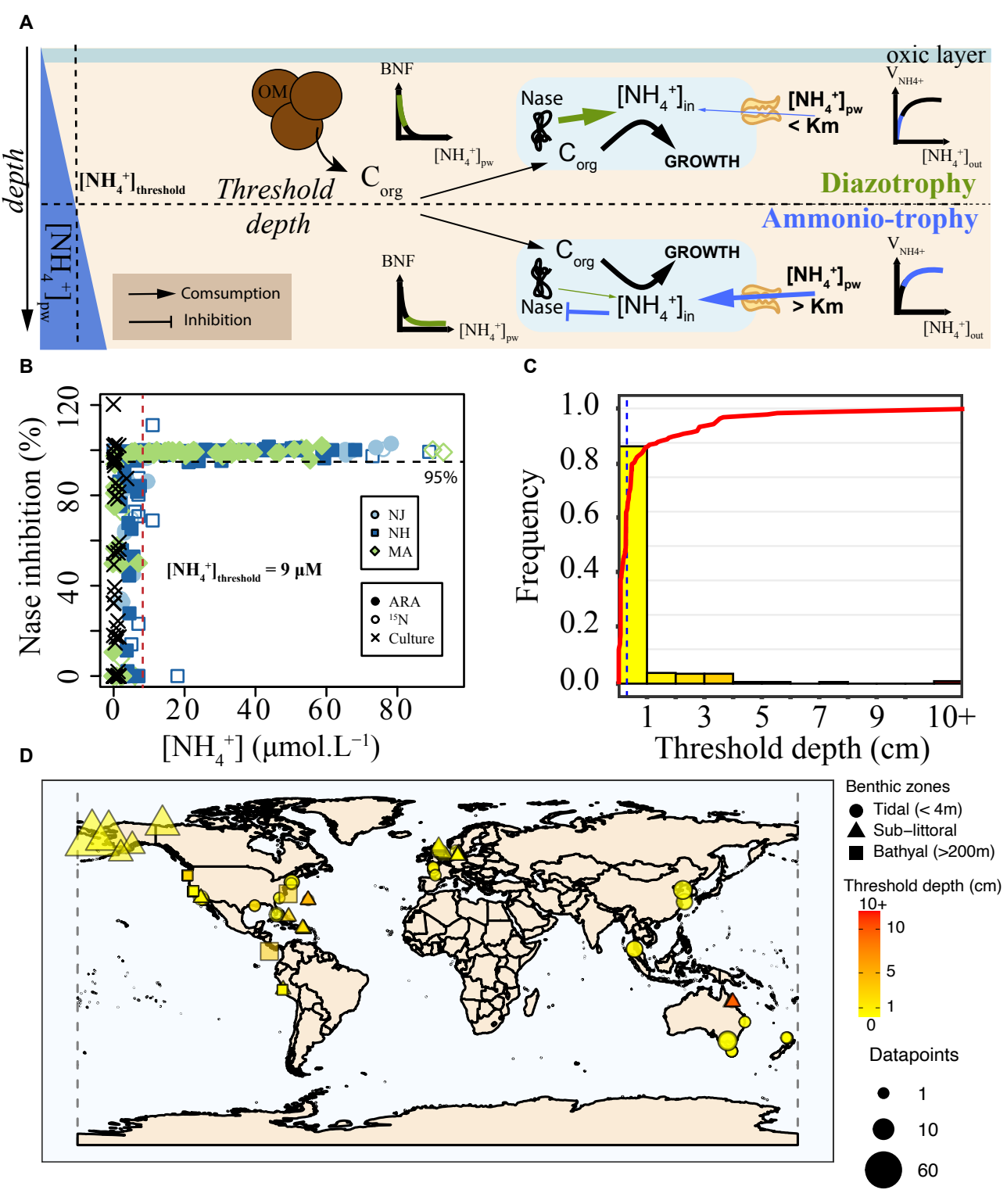
A
depth
oxic layer
OM
BNF
[NH4+]pw
Nase
[NH4+]in
[NH4+]pw
< Km
Corg
GROWTH
VNH4+
[NH4+]out
[NH4+]threshold
Threshold
depth
Corg
Diazotrophy
Ammonio-trophy
BNF
[NH4+]pw
Corg
GROWTH
Nase
[NH4+]in
[NH4+]pw
> Km
VNH4+
[NH4+]out
Comsumption
Inhibition
B
Nase inhibition (%)
95%
NJ
NH
MA
[NH4+]threshold = 9 µM
ARA
15N
Culture
[NH4+] (µmol.L−1)
C
Frequency
Threshold depth (cm)
D
Benthic zones
Tidal (< 4m)
Sub−littoral
Bathyal (>200m)
Threshold depth (cm)
10+
10
5
1
0
Datapoints
1
10
60

Table 1 : Sediments carbon and nitrogen compositions

	%C[1]	SD*$_{intra}$ (n=10)	%N	SD$_{intra}$ (n=10)	C:N[2]	SD$_{intra}$ (n=10)	$\delta^{13}C$	SD$_{intra}$ (n=10)	$\delta^{15}N$	SD$_{intra}$ (n=10)
Barnaget Bay (NJ)	6.7	3.4	0.30	0.18	28.3	7.0	-27.7	0.4	2.2	0.9
*SEM** (n=2)*	*0.3*	*0.1*	*0.01*	*0.01*	*0.4*	*2.6*	*0.2*	*0.1*	*0.2*	*0.6*
Great Bay (NH)	5.4	0.9	0.43	0.07	14.7	0.5	-15.5	0.2	5.1	0.4
SEM (n=4)	*0.2*	*0.1*	*0.01*	*0.01*	*0.1*	*0.1*	*0.1*	*0.1*	*0.1*	*0.2*
Sippewissett Marsh (MA)	22.2	6.9	1.74	0.53	14.9	0.3	-18.1	0.4	3.2	0.4
SEM (n=4)	*1.1*	*0.5*	*0.08*	*0.05*	*0.2*	*0.0*	*0.1*	*0.2*	*0.1*	*0.1*

[1]. %C and %N are on a mass basis relative to oven-dried sediments ($g_{element}.g_{ODW}^{-1}$). [2]. C:N are molar ratio.

*SD_{intra} represents sample heterogeneity, as the SD of 10 replicates taken from the same sample over multiple timepoints and averaged per sediment geography.

**SEM represents the standard error of the mean for each sediment geography.

Supplementary Information for: Ammonium sensitivity of biological nitrogen fixation in anaerobic diazotrophs and coastal salt marsh sediments.

Romain Darnajoux[1], Linta Reji[1], Xin Rei Zhang[1,2], Katja E. Luxem[1], and Xinning Zhang[1, 2]

[1]Department of Geosciences, Princeton University, Princeton, 08544, NJ, USA

[2]High Meadows Environmental Institute, Princeton University, Princeton, 08544, NJ, USA

Corresponding author: RD and XZ

ORCID: RD: 0000-0002-4996-0067, XZ: 0000-0003-2763-1526, KEL: 0000-0001-7310-0668, LR: 0000-0002-1337-6782

SUPPLEMENTARY METHODS:

1) *Method S1: Contribution of BNF to new biomass production in pure culture of Desulfovibrio vulgaris var. Hildenborough (DvH)*

In order to estimate the contribution of BNF to new biomass production between two time points (Δt) during incubations (see Fig.1B), Eq. [1] expresses the new biomass created from measured BNF input ($dn_{cell,BNF}$) over total biomass increase ($dn_{cell,tot}$)

[eq 1] % BNF contribution = $[dn_{cell,BNF}/dn_{cell,tot}]_{\Delta t}$

Newly fixed N is approximated based on the amount of ethylene produced between timepoints using Eq. [2],

[eq 2] $dn_{N,BNF} = A*dppm_E$

and the total increase in biomass is approximated using the change in optical density as shown by Eq. [3]

[eq 3] $dn_{cell} = B*dOD_{600}$

In these equations, $dn_{N,BNF}$ is the quantity of N in mol, $dppm_E$ is the equivalent quantity of ethylene reduced in ppm v/v in headspace, dn_{cell} is the change in cell number, dOD_{600} is the change in turbidity at 600nm, and A and B are undetermined proportionality factors. The relative contribution of BNF to biomass production was derived from the control experiment without NH_4^+ addition, allowing us to estimate the parameter A using a rearrangement of Eq. [2]. The quantity of cells that originates from newly fixed N for any sample between two time points can now be expressed using [Eq.4].

[eq 4] $dn_{cell,BNF,\Delta t} = dn_{N,BNF,\Delta t}*[dn_{N,BNF}/dn_{cell,BNF}]_{ctrl}$

We substitute Eq. 4, 2 and 3 in 1, and after simplification of A and B, we can express the BNF contribution between each time point for data in Figure 1B using [Eq.5]

[eq 5] % BNF contribution = $[dppm_E/dOD_{600}]_{\Delta t,addition}$ /$[dppm_E/dOD_{600}]_{\Delta t,ctrl}$

2) Method S2: Calculation of residual NH_4^+ in media after biomass uptake

The residual ammonium concentration in medium after uptake for growth (presented in Supplementary Fig. S7) can be expressed as the initial quantity of NH_4^+ ($n_{NH4,media,0}$) minus the sum of the incremental quantities used by cells for growth over time ($dn_{NH4,cell,\Delta t}$):

[eq 6] $[NH_4^+]_t = n_{NH4,media} / V_{media} = (n_{NH4,media,0} - \sum dn_{NH4,cell,\Delta t}) / V_{media}$

Where V_{media} is the volume of media. For every Δt, the quantity of cells grown from media NH_4^+ ($dn_{cell,NH4,\Delta t}$) can be derived by rearranging Eq.[1] as the contribution of NH_4^+ to growth (estimated from BNF contribution to growth) multiplied by total cellular growth ($dn_{cell,tot,\Delta t}$):

[eq 7] $dn_{cell,NH4,\Delta t} = (1- \%\ BNF\ contribution_{,\Delta t}) * dn_{cell,tot,\Delta t}$

The amount of nitrogen necessary to produce 1 OD unit of biomass can be calibrated using the first growth plateau in sub-replete condition (*i.e.,* second lag-phase before the onset of BNF, see growth curve @ $[NH_4^+]$ =500 µM in main text Fig.1A), using Eq. [8]:

[eq 8] $dn_{NH4,cell,\Delta t} = dn_{cell,NH4,\Delta t} / [n_{NH4,media,0} / n_{cell,NH4,plateau}]_{sub\text{-}replete}$

allowing the calculation of ammonium uptake at each time Δt ($dn_{NH4,cell,\Delta t}$), and thus residual $[NH_4^+]$ using Eq.[6]. after simplification of B (from eq. [3]) and V_{media} (assuming constant media volume V_{media} over the experiment) using Eq. [9]:

[eq 9]

$[NH_4^+]_t = [NH_4^+]_{,media,0} - \sum (1- \%\ BNF\_contribution_{,\Delta t}) * dOD_{600,\Delta t} / ([NH_4^+]_{media,0} / OD_{600,plateau})_{sub\text{-}replete}$

SUPPLEMENTARY FIGURES

Figure S1

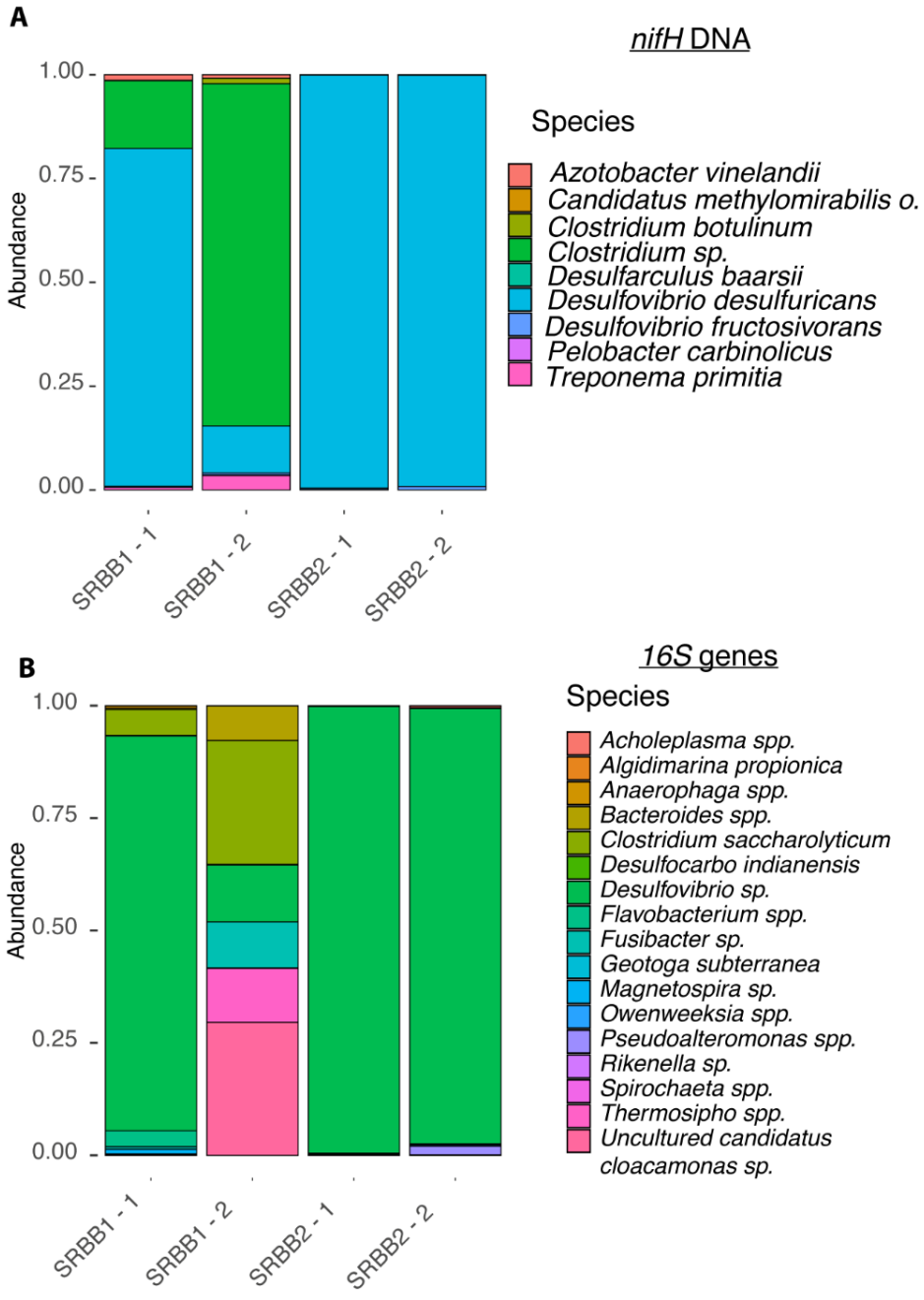

Figure S1: Microbial composition of SRBB1 and SRBB2 consortia based on *nifH* genes (A) and *16S* rRNA genes (B). Each consortium was cultivated in two replicates under the same conditions as in the experiment shown in Figure 2B. Nitrogen fixers in the consortia were dominated by *Desulfovibrio sp.*

FIGURE S2

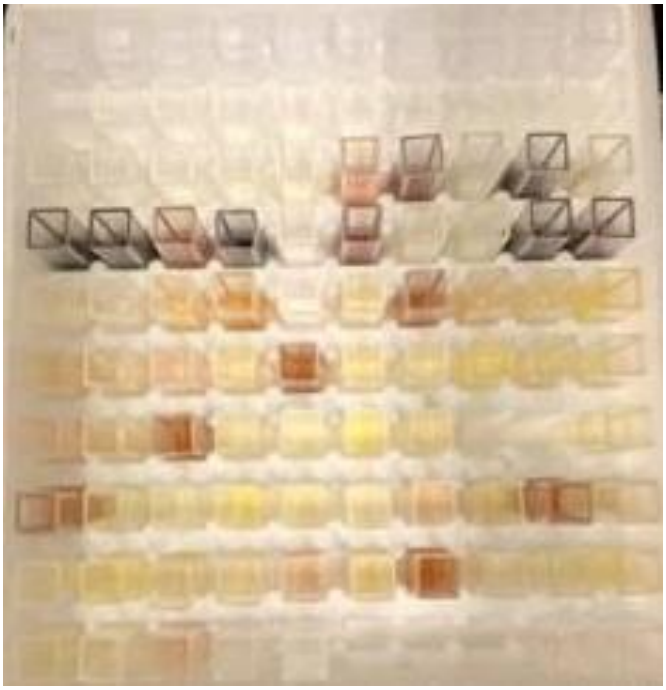

Figure S2: **Picture of filtered slurry samples after reaction with the o-phthalaldehyde (OPA) reagent**. The samples in the bottom of this picture are from early time points of the sediment ARA incubation, and show the white to yellow color expected in the OPA method. In the top of the picture, we see that the samples taken from 5 incubations after addition of ammonium (#4, #6, #7, #9, and #10) show abnormal dark orange to purple hues, even after 8-fold dilutions. No similar red-purple hues were observed with ^{15}N incubation samples.

FIGURE S3

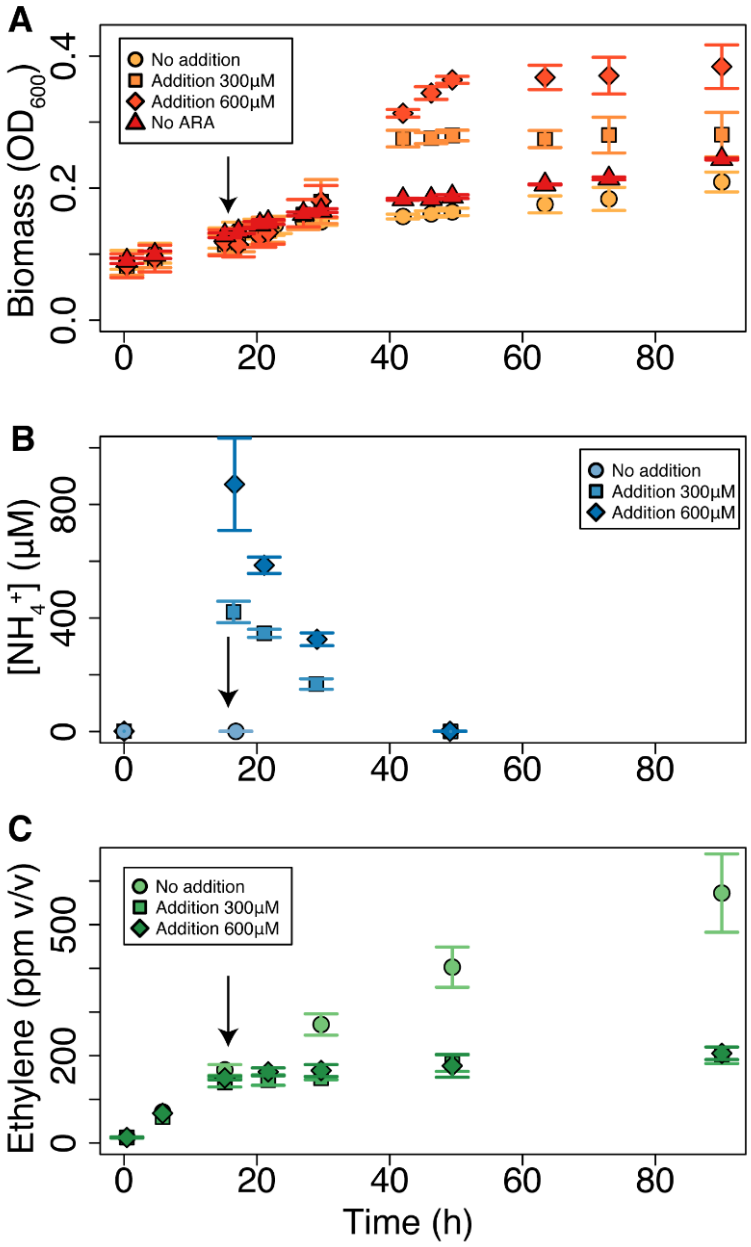

Figure S3: **Effect of ammonium concentration on the acetylene reduction activity of *Desulfovibrio vulgaris* var. Hildenbourough (DvH)**. The change in biomass (A), ammonium concentration (B), and headspace ethylene was monitored during incubation (C) with (square and diamond) and without (circle) added NH_4^+. In panel A, comparison of growth rate and yield with and without addition of ~2.5%v/v acetylene (circle vs. triangle) illustrates limited inhibition (30-40% decrease in growth rate) of acetylene on DvH. Error bars are standard error of three technical replicates.

FIGURE S4

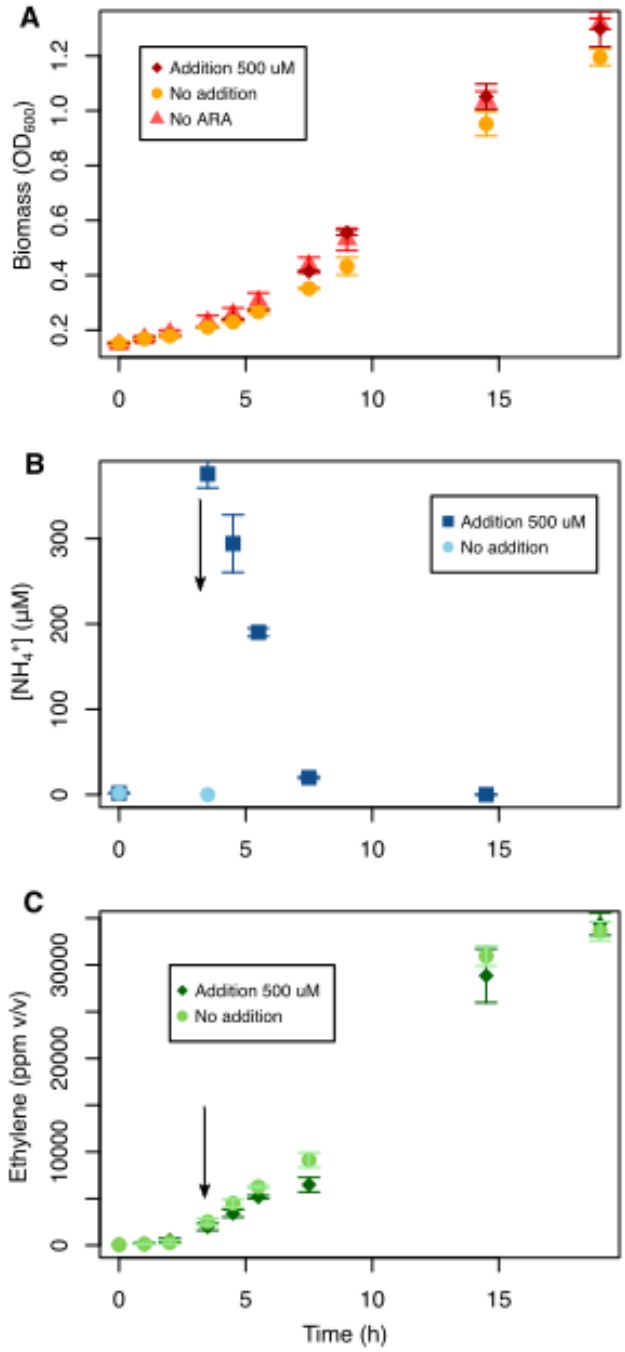

Figure S4: **Effect of ammonium concentration on the acetylene reduction activity of *Clostridium pasteurianum* strain W3 (Cp)**. The change in biomass (A), ammonium concentration (B), and headspace ethylene was monitored during incubation (C) with (square and diamond) and without (circle) added NH_4^+. In panel A, comparison of growth rate and yield with and without addition of ~2.5%v/v acetylene (circle vs. triangle) illustrates limited inhibition (~5% decrease in growth rate) of acetylene on *Cp*. Error bars are standard error of three technical replicates.

FIGURE S5

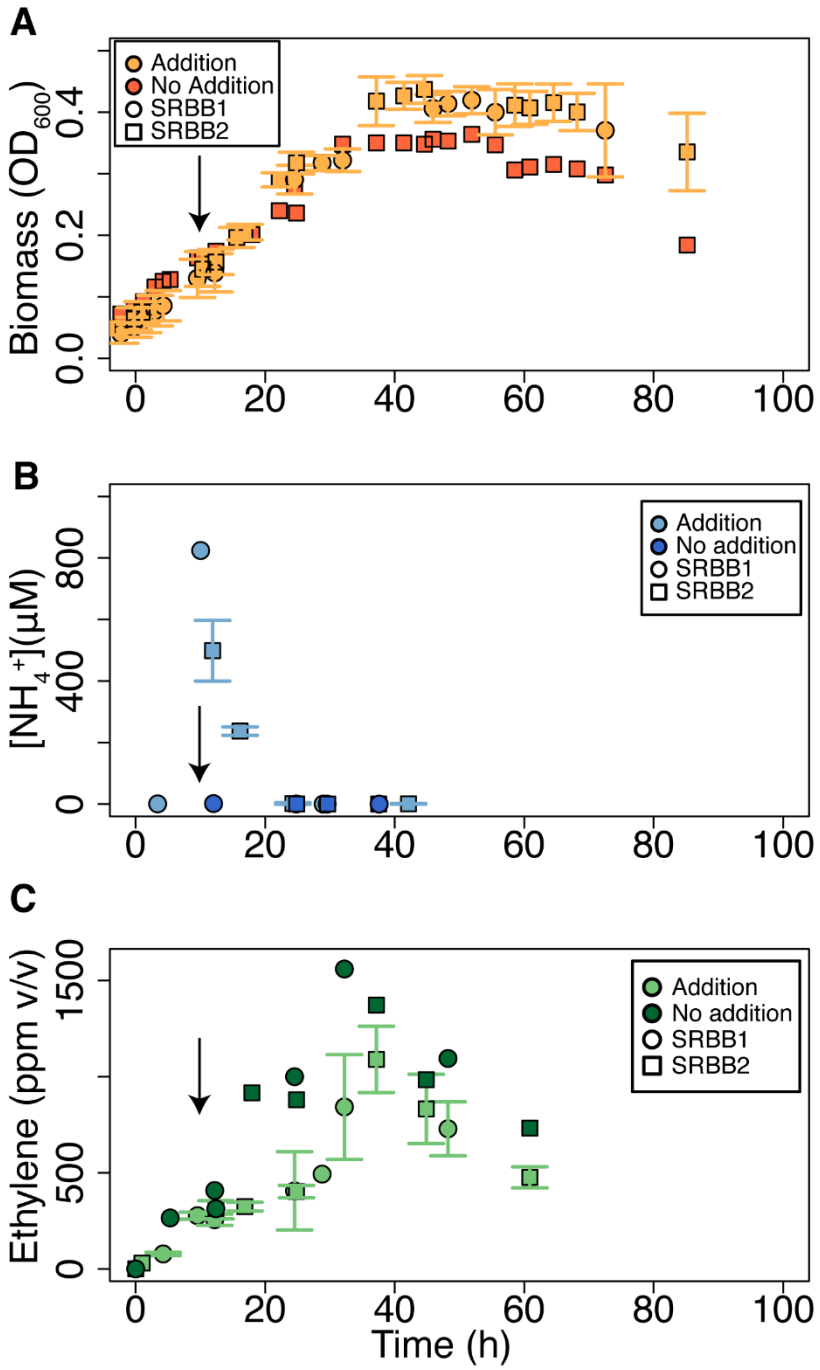

Figure S5: **Effect of ammonium concentration on acetylene reduction activity in two enrichment cultures from Barnegat Bay salt marshes sediments** (SRBB1 and SRBB2, see main text M&M). The evolution of biomass (A), ammonium concentration (B), and headspace ethylene (C) during ARA experiments with (dark) and without (light) added NH_4^+ are shown. Error bars show the standard error of three technical replicates.

Figure S6

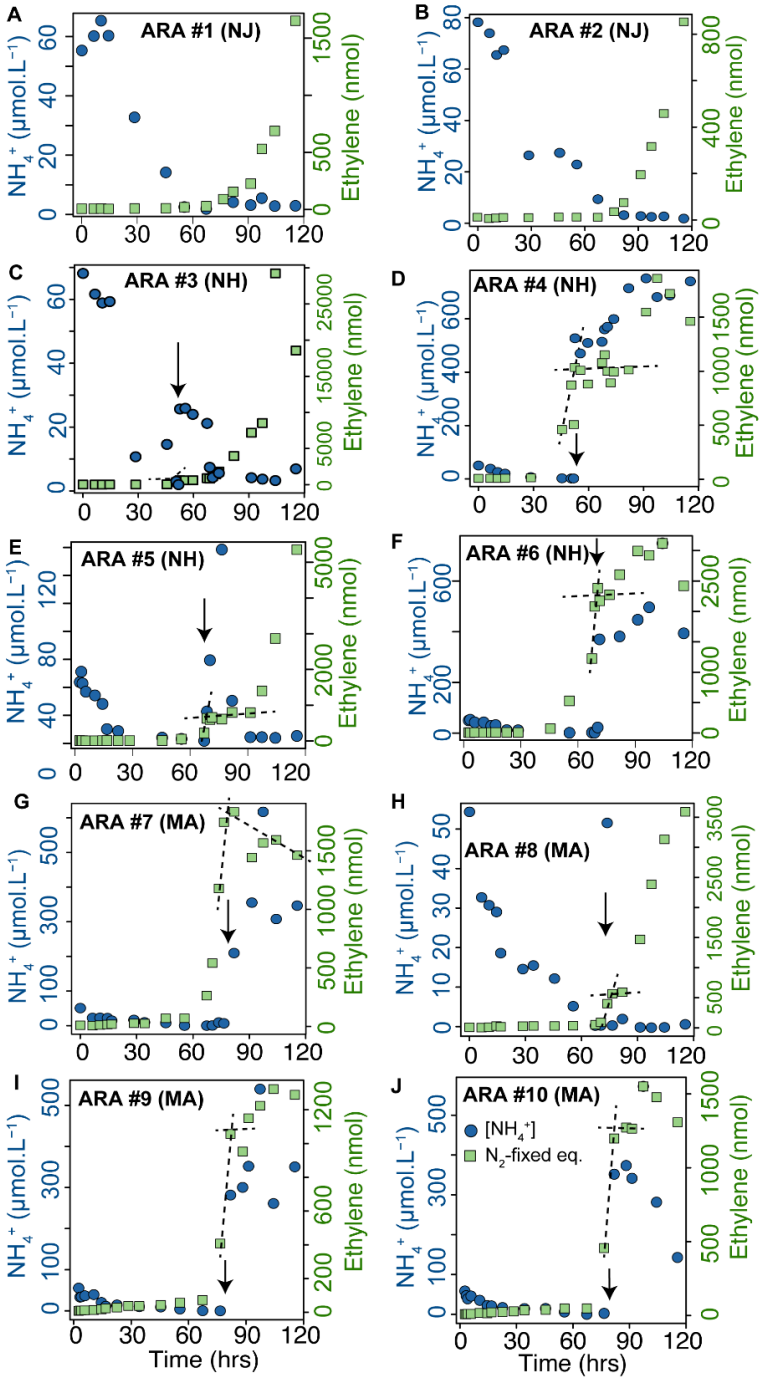

Figure S6: **Effect of ammonium concentration on the acetylene reduction activity of salt-marsh sediments.** Dissolved [NH_4^+] (blue circles) and Biological Nitrogen Fixation (BNF) activity evaluated using Acetylene Reduction Assay (green squares) over time in salt marsh sediments from Barnegat Bay, New Jersey (NJ, A and B), Great Bay, New Hampshire (NH, C to F), and Sippewissett, Massachusetts (MA, G to J) in slurry incubations with no NH_4^+ amendment (A and B) and with NH_4^+ additions (C to J). Additions are indicated with arrows. Dashed lines illustrate interpolation of the BNF rate before and after NH_4^+ addition to estimate the time to BNF inhibition (T_R).

Figure S7

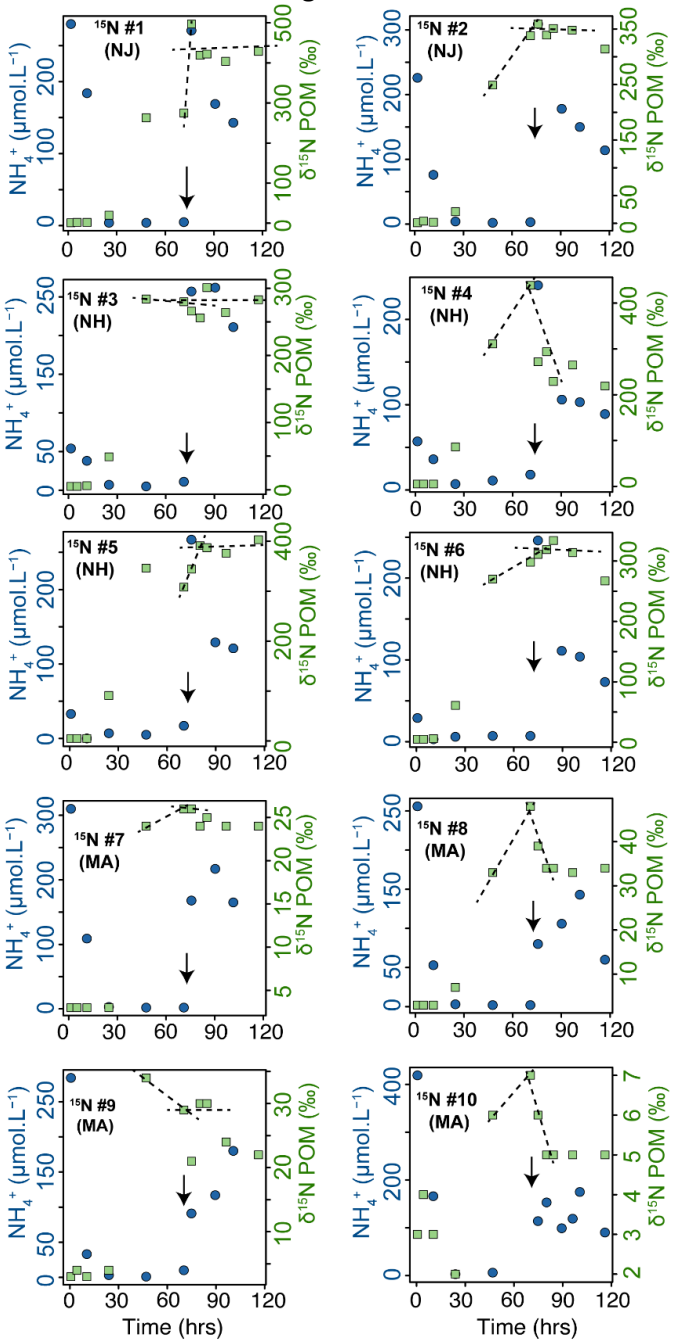

Figure S7: **Effect of ammonium concentration on ^{15}N- Biological Nitrogen Fixation (BNF) activity in salt-marsh sediments.** Dissolved [NH_4^+] (blue circles) and BNF activity evaluated using ^{15}N tracer experiment (green squares) over time in salt marsh sediment from Barnegat Bay, New Jersey (NJ, A and B), Great Bay, New Hampshire (NH, C to F), and Sippewissett, Massachussett (MA, G to J) in slurry incubations with no NH_4^+ amendment (A and B) and with NH_4^+ additions (C to J). Additions are indicated with arrows. All sediment samples except #3 to #6 received addition of ammonium before starting the experiments. Dashed lines illustrate the interpolation of the BNF rate before and after NH_4^+ addition that was used to estimate the time to BNF inhibition (T_R).

Figure S8

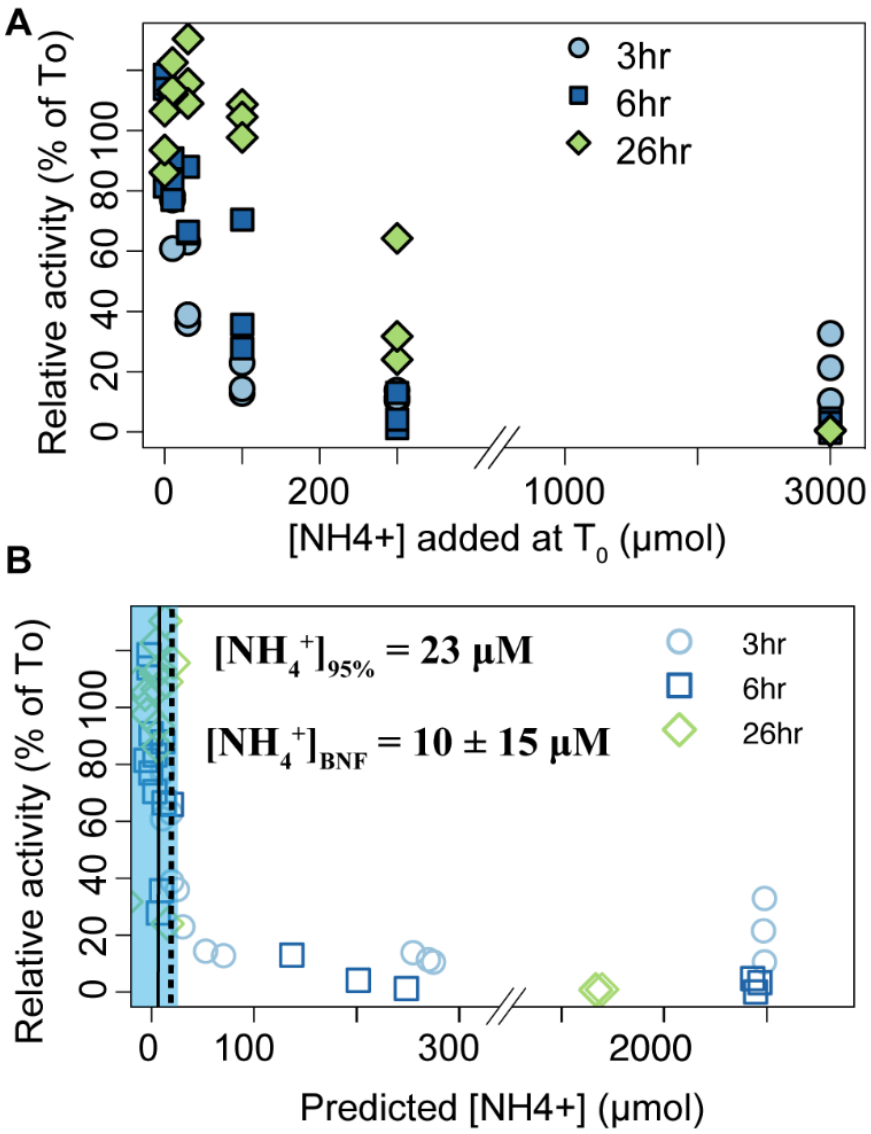

Figure S8. Effect of timing and initial concentration on residual ammonium media concentration and Biological Nitrogen Fixation (BNF) activity. Relative BNF activity measured using Acetylene Reduction Assay at 3h, 6h and 26h after additions of NH_4^+ (to reach concentration of 10, 30, 100, 300, and 3,000 µM, see main text Figure 1B) compared to BNF activity before NH_4^+ addition for *Desulfovibrio vulgaris* var. Hildenborough initially grown under N_2-fixing conditions as a function of initially added concentration (A) and calculated residual [NH_4^+] in the media at the time of sampling (B), as calculated according to Supplementary Methods S2. Symbols represent individual samples from a single experiment. Blue boxes indicate the range of ammonium values showing detectable BNF (>20%), the black lines indicate the average values, and dotted lines the 95-percentile (*i.e.*, threshold value).

FIGURE S9

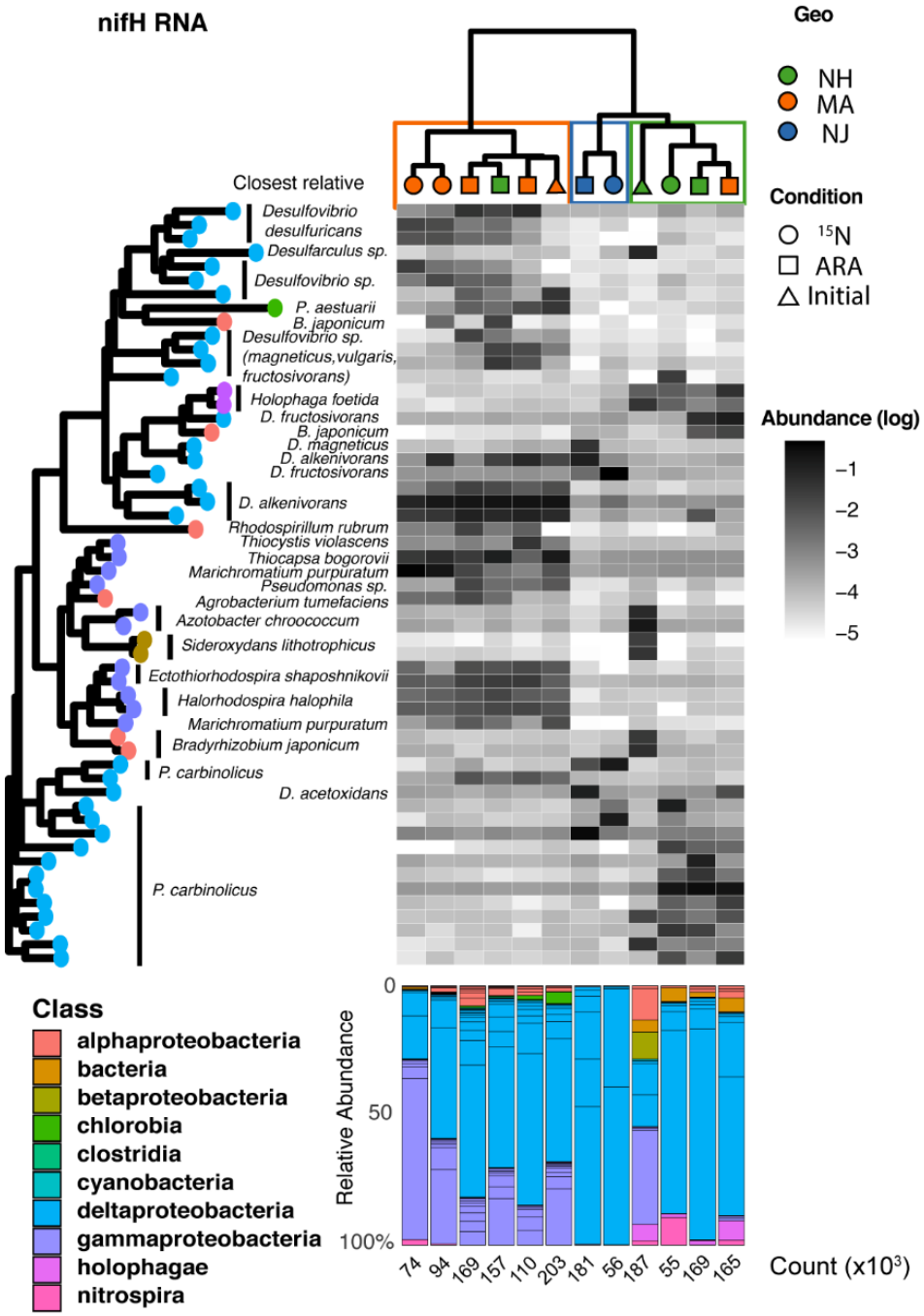

Figure S9: Microbial composition of diazotroph community in salt marsh sediment incubations. Heatmap of *nifH* RNA relative abundance (log-scale) at the end of incubation with class-level information for the 200 first OTUs (bottom bar plot, > 85 % total abundance) and detailed phylogeny and closest relatives for the most abundant sequences (left panel, OTUs with relative abundance >0.2% & total count >1000, n=55). Hierarchical clustering of individual sediment samples based on *nifH* composition (top left of panel) shows the relationship between sample *nifH* RNA composition, incubation condition (ARA vs. ^{15}N), and geographical origin of the sediments.

FIGURE S10

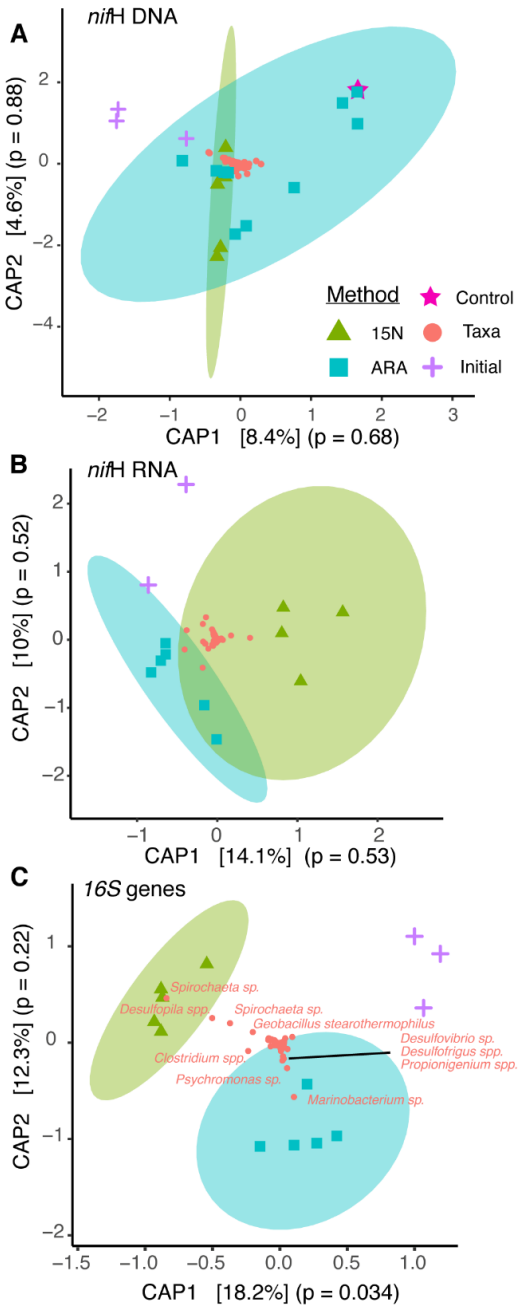

Figure S10: **Effect of acetylene (2.5%v/v) on the microbiomes of sediments after five day in slurry incubation.** Discrimination analysis using Canonical Analysis of Principal coordinates (using Bray-Curtis distance) on (A) *nifH* genes, (B) *nifH* transcript, et (C) *16S* rRNA genes. Axes show the percent of variance explained and the statistical significance for each explanatory axis as estimated using permutation Anova. Blue and green disc highlight the 95% confidence ellipses. Results were unchanged when we control for the origin of the sediment (NJ, NH, and MA), or when we remove the initial and control data. In panel C, species that are over-represented in one group are listed in red.

FIGURE S11

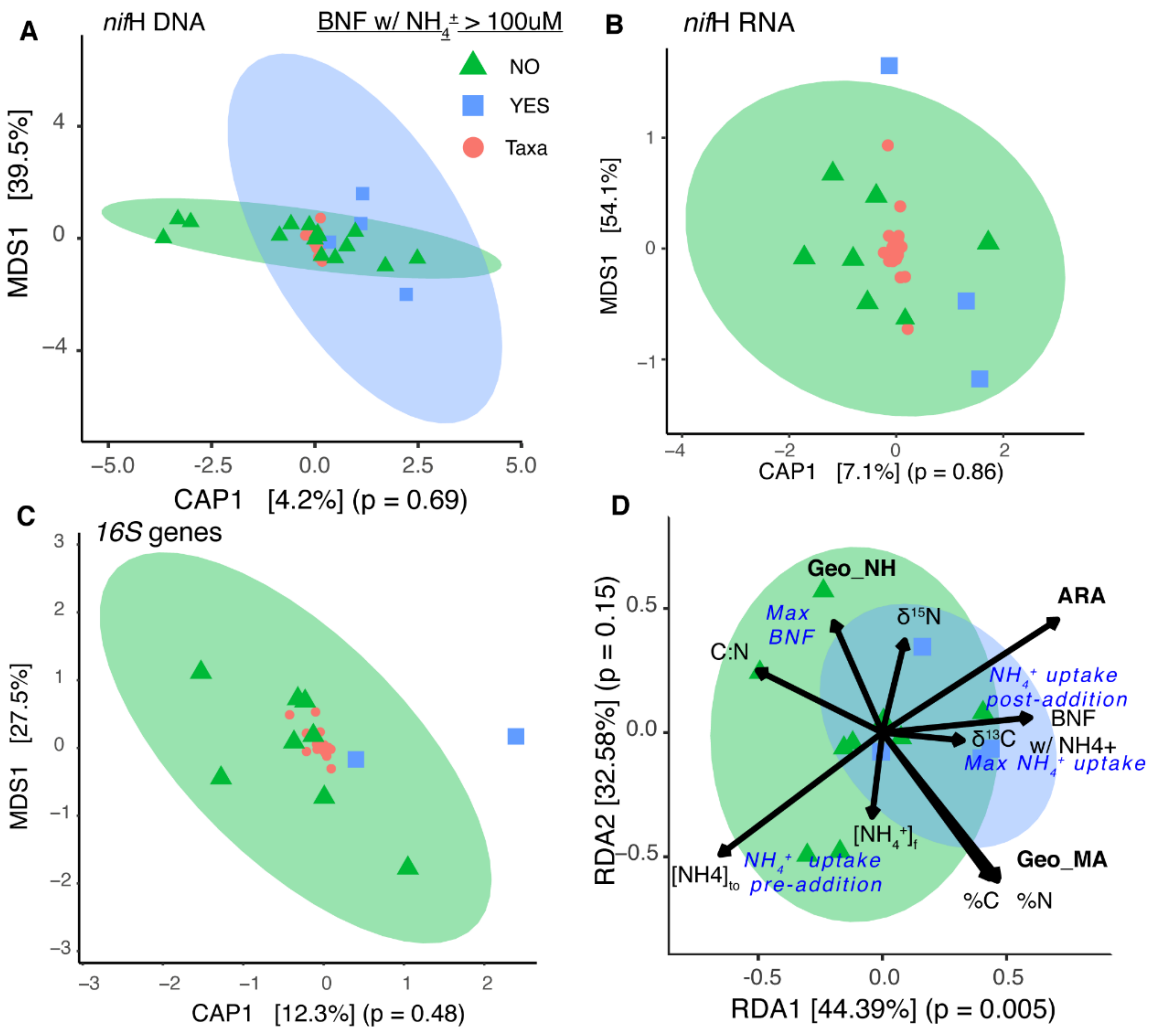

Figure S11: Discrimination analysis of samples showing increase ethylene production at high ammonium. Canonical Analysis of Principal Coordinates on Bray-Curtis distance of microbial communities for (A) *nifH* genes (n=4), (B) *nifH* transcript (n=3) and (C) *16S* genes (n=2), and Redundancy Analysis on normalized biogeochemical data (D, n=4) on samples (total 4/20) showing increased headspace ethylene with post addition $[NH_4^+]$ > 100µM. Axes show the percent of variance explained and the statistical significance for each explanatory axis as estimated using permutation Anova. Results were unchanged when controlled for the origin of the sediment (NJ, NH, and MA) or the method used to assess BNF activity (^{15}N tracer vs. Acetylene Reduction Assay). Blue and green disc represent the 95% confidence ellipses for each group. In panel D, variables in bold are significantly influencing the model.

FIGURE S12

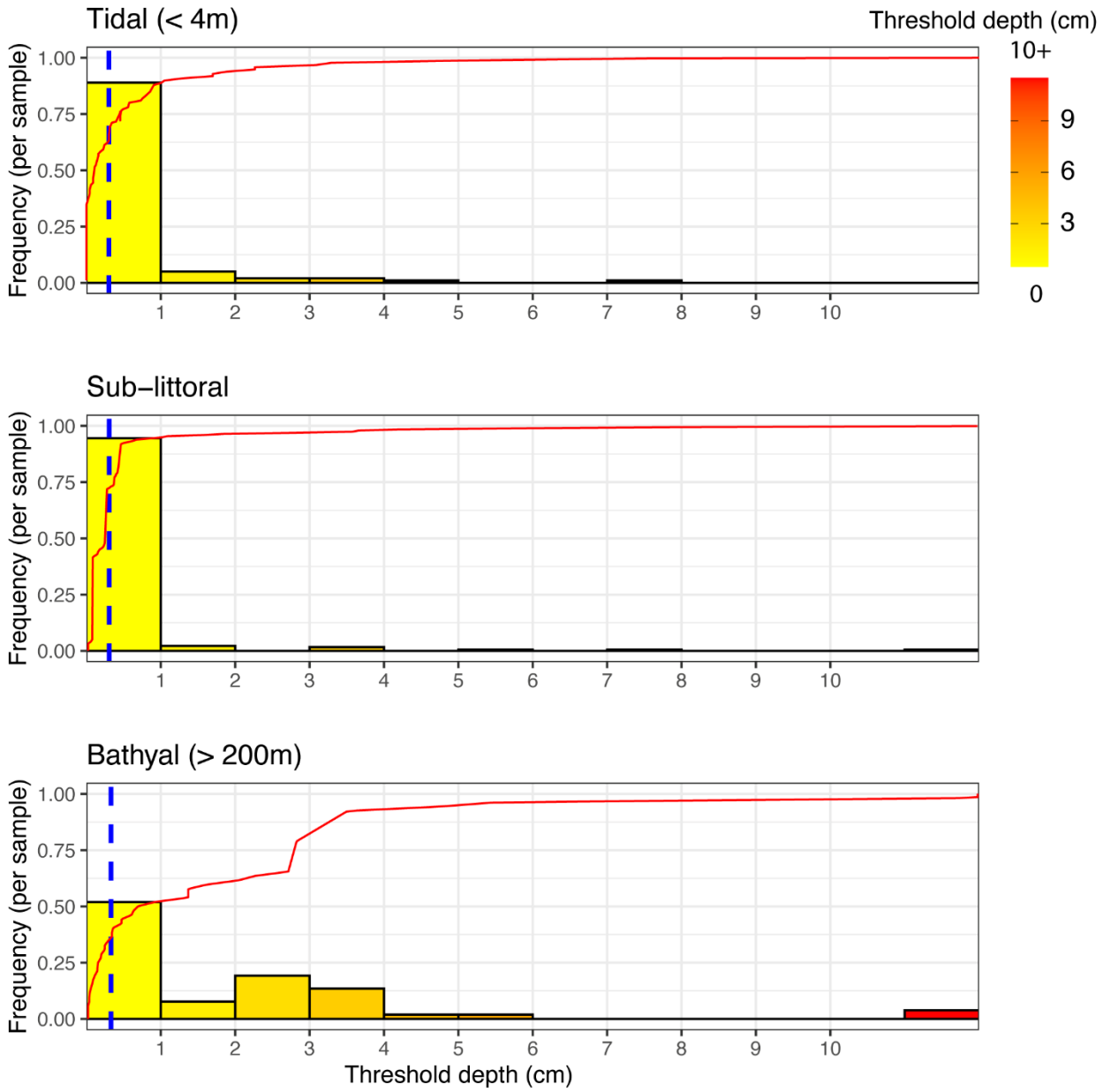

Figure S12: Frequency distribution of threshold depth per benthic zones. Threshold depth (*i.e.*, depth at which $[NH_4^+]_{threshold}$ was reached) were derived from literature review of 26 study (151 sites, 334 replicates, see Table S1). Benthic zones were separate according to reported water depth as tidal (< 4 m, n= 64), sub-littoral (between 4 and 200 m, n=47), and bathyal (> 200 m, n=40) The red lines represent cumulative frequencies, and the dashed vertical line represent the median value.

SUPPLEMENTARY DISCUSSION

OBSERVATIONS:

We identified four instances that could be interpreted to suggest that nitrogenase activity is not sensitive to high ammonium concentrations, contrary to the main conclusion of our work. Here, in this Supplementary Discussion, we describe these observations and why we have concluded that they are most likely misleading artefacts rather than a true biological phenomenon.

Several filtered supernatant aliquots representing several timepoints sampled from five sediment incubations assessed by ARA (#4, #6, #7, #9, #10, Fig. S5) after NH_4^+ addition exhibited irregular coloration (red-black instead of yellow) during the OPA procedure, even after 8-fold dilution (Fig. S2). In four of these five samples (two each from the NH and MA salt marshes), an increase in headspace ethylene was observed ~ 10h after an initial plateau following NH_4^+ addition, even though measured [NH_4^+] remained > 100 μM at this time (Fig. S5 #4, #6, #9&#10). These observations of increased headspace ethylene levels were limited to a few timepoints, showed a step-like behavior in two of the four occurrences, and stopped before the end of the experiment (see Fig. S5). For four of the eight ARA sediment samples (two each from NH and MA salt marshes) spiked with NH_4^+, BNF rates also resumed within ~ 10h after addition, but ambient NH_4^+ was drawn down to near background levels ([NH_4^+] < 10 μM, Main article Fig. 2C, Fig. S5) within this timeframe, likely due to assimilatory or dissimilatory biological activities. Together, these observations suggest that the "measured" ammonium concentration calculated based on sample absorbance during the OPA assay might be incorrect in these samples. Indeed, two of these four samples even showed an increase in NH_4^+ concentration in the absence of further exogenous ammonium addition. Importantly, none of the 10 sediment incubations assayed using the ^{15}N tracer method, which directly reflect BNF activity, showed any evidence of a resumption of BNF activity after NH_4^+ amendment, and post addition NH_4^+ concentration never decreased below 50 μM (Fig. S6).

DISCRIMINATION ANALYSES:

To confirm that the microbiome in samples with abnormally colored OPA samples (5 out of 20 experiments, Fig. S5), where we observed increases in headspace ethylene concentrations coincident with the appearance of high

ammonium (>100 uM), is similar to the other samples, we performed a discriminant analyses on the *nifH* microbiome data (CAP on Bray-Curtis dissimilarities, Fig. S10) from our ARA and ^{15}N incubations. We could not distinguish these four samples from others exhibiting the classical response of BNF inhibition by ammonium based on their microbial composition (*nifH* and *16S* genes), even when controlling for the geographic origin of sediments as the covariate (Fig. S10 panel A-C). This implies that there is no single organism or assemblage of diazotrophs, as assessed by *nifH* or 16S at the end of incubation, that can easily explain our anomalous observations of BNF. We also found good correlation between the presence of ethylene production at high NH_4^+ concentration and the maximum NH_4^+ depletion rate using redundancy analysis on the biogeochemical data (Fig. S10 panel D), but the high confoundedness between variables prevents a more definitive interpretation.

SUMMARY AND CONCLUSION:

In four instances from two sites (MA and NH), we found results that could be interpreted as evidence that nitrogenase activity is not sensitive to high ammonium concentrations (Fig. S5 #4, #6, #9 & #10). This could suggest changes in ammonium uptake and regulatory mechanisms of BNF in a suite of specialized diazotrophs. There are, however, several arguments against such a conclusion; i) in all of these ARA samples, BNF activity initially stopped for 7-20 h directly after ammonium addition, indicating the active diazotrophs were sensitive to ammonium, ii) ethylene production resumed for less than 30h with lower activity, step-wise increase, and all samples stopped producing ethylene by the end of the incubation, iii) no OTUs based on *16S* and *nifH* analyses could be specifically linked to these four samples, and iv) we did not found evidence of similar phenomena in any of our ^{15}N tracer incubations. Possible explanations for anomalous findings in the 4 samples range from artifacts of long incubation (5 days), where high biomass increase could foster the development of microniches of depleted ammonium, methodological flaws (OPA measurement of ammonium, headspace sampling, agitation), and human error. After careful consideration, these specific data points were annotated where included in the main article (Figure 3B) and removed from further analyses.